Genomic analysis of European Drosophila melanogaster populations reveals longitudinal structure, continent-wide selection, and previously unknown DNA viruses

Martin Kapun, Maite G Barrón, Fabian Staubach, Darren J Obbard, R Axel W. Wiberg, Jorge Vieira, Clément Goubert, Omar Rota-Stabelli, Maaria Kankare, María Bogaerts-Márquez, et al.

Genomic analysis of European *Drosophila melanogaster* populations reveals longitudinal structure, continent-wide selection, and previously unknown DNA viruses

Martin Kapun[1,2,3,4,†,*], Maite G. Barrón[1,5,*], Fabian Staubach[1,6,§], Darren J. Obbard[1,7], R. Axel W. Wiberg[1,8,9], Jorge Vieira[1,10,11], Clément Goubert[1,12,13], Omar Rota-Stabelli[1,14], Maaria Kankare[1,15,§], María Bogaerts-Márquez[1,5], Annabelle Haudry[1,12], Lena Waidele[1,6], Iryna Kozeretska[1,16,17,], Elena G. Pasyukova[1,18], Volker Loeschcke[1,19], Marta Pascual[1,20], Cristina P. Vieira[1,10,11], Svitlana Serga[1,16], Catherine Montchamp-Moreau[1,21], Jessica Abbott[1,22], Patricia Gibert[1,12], Damiano Porcelli[1,23], Nico Posnien[1,24], Alejandro Sánchez-Gracia[1,20], Sonja Grath[1,25], Élio Sucena[1,26,27], Alan O. Bergland[1,28,§], Maria Pilar Garcia Guerreiro[1,29], Banu Sebnem Onder[1,30], Eliza Argyridou[1,25], Lain Guio[1,5], Mads Fristrup Schou[1,19,22], Bart Deplancke[1,31], Cristina Vieira[1,12], Michael G. Ritchie[1,8], Bas J. Zwaan[1,32], Eran Tauber[1,33], Dorcas J. Orengo[1,20], Eva Puerma[1,20], Montserrat Aguadé[1,20], Paul S. Schmidt[1,34,§], John Parsch[1,25], Andrea J. Betancourt[1,35], Thomas Flatt[1,2,3,†,*,§], Josefa González[1,5,†,*,§]

[1] The European *Drosophila* Population Genomics Consortium (*DrosEU*). [2] Department of Ecology and Evolution, University of Lausanne, CH-1015 Lausanne, Switzerland. [3] Department of Biology, University of Fribourg, CH-1700 Fribourg, Switzerland. [4] Current affiliations: Department of Evolutionary Biology and Environmental Sciences, University of Zürich, CH-8057 Zürich, Switzerland; Division of Cell and Developmental Biology, Medical University of Vienna, AT-1090 Vienna, Austria. [5] Institute of Evolutionary Biology, CSIC- Universitat Pompeu Fabra, Barcelona, Spain. [6] Department of Evolutionary Biology and Ecology, University of Freiburg, 79104 Freiburg, German. [7] Institute of Evolutionary Biology, University of Edinburgh, Edinburgh, United Kingdom. [8] Centre for Biological Diversity, School of Biology, University of St. Andrews, St Andrews, United Kingdom. [9] Department of Environmental Sciences, Zoological Institute, University of Basel, Basel, CH-4051, Switzerland.[10] Instituto de Biologia Molecular e Celular (IBMC) University of Porto, Porto, Portugal. [11] Instituto de Investigação e Inovação em Saúde (I3S), University of Porto, Porto, Portugal. [12] Laboratoire de Biométrie et Biologie Evolutive, UMR CNRS 5558, University Lyon 1, Lyon, France. [13] Department of Molecular Biology and Genetics, 107 Biotechnology Building, Cornell

University, Ithaca, New York 14853, USA. [14] Research and Innovation Centre, Fondazione Edmund Mach, San Michele all' Adige, Italy. [15] Department of Biological and Environmental Science, University of Jyväskylä, Jyväskylä, Finland. [16] General and Medical Genetics Department, Taras Shevchenko National University of Kyiv, Kyiv, Ukraine. [17] State Institution National Antarctic Center of Ministry of Education and Science of Ukraine, 16 Taras Shevchenko Blvd., 01601, Kyiv, Ukraine. [18] Laboratory of Genome Variation, Institute of Molecular Genetics of RAS, Moscow, Russia. [19] Department of Bioscience - Genetics, Ecology and Evolution, Aarhus University, Aarhus C, Denmark. [20] Departament de Genètica, Microbiologia i Estadística, Facultat de Biologia and Institut de Recerca de la Biodiversitat (IRBio), Universitat de Barcelona, Barcelona, Spain. [21] Laboratoire Evolution, Génomes, Comportement et Ecologie (EGCE) UMR 9191 CNRS - UMR247 IRD - Université Paris Sud - Université Paris Saclay. 91198 Gif sur Yvette Cedex, France. [22] Department of Biology, Section for Evolutionary Ecology, Lund, Sweden. [23] Department of Animal and Plant Sciences, Sheffield, United Kingdom. [24] Universität Göttingen, Johann-Friedrich-Blumenbach-Institut für Zoologie und Anthropologie, Göttingen, Germany. [25] Division of Evolutionary Biology, Faculty of Biology, Ludwig-Maximilians-Universität München, Planegg, Germany. [26] Instituto Gulbenkian de Ciência, Oeiras, Portugal. [27] Departamento de Biologia Animal, Faculdade de Ciências da Universidade de Lisboa, Lisboa, Portugal. [28] Department of Biology, University of Virginia, Charlottesville, VA, USA. [29] Departament de Genètica i Microbiologia, Universitat Autònoma de Barcelona, Barcelona, Spain. [30] Department of Biology, Faculty of Science, Hacettepe University, Ankara, Turkey. [31] Laboratory of Systems Biology and Genetics, EPFL-SV-IBI-UPDEPLA, CH-1015 Lausanne, Switzerland. [32] Laboratory of Genetics, Department of Plant Sciences, Wageningen University, Wageningen, Netherlands. [33] Department of Evolutionary and Environmental Biology and Institute of Evolution, University of Haifa, Haifa, Israel. [34] Department of Biology, University of Pennsylvania, Philadelphia, USA. [35] Institute of Integrative Biology, University of Liverpool, Liverpool, United Kingdom.

[†] Co-correspondence: martin.kapun@uzh.ch, thomas.flatt@unifr.ch, josefa.gonzalez@ibe.upf-csic.es

[*] These authors contributed equally to this work

[§] Members of the *Drosophila* Real Time Evolution (Dros-RTEC) Consortium

Abstract

Genetic variation is the fuel of evolution, with standing genetic variation especially important for short-term evolution and local adaptation. To date, studies of spatio-temporal patterns of genetic variation in natural populations have been challenging, as comprehensive sampling is logistically difficult, and sequencing of entire populations costly. Here, we address these issues using a collaborative approach, sequencing 48 pooled population samples from 32 locations, and perform the first continent-wide genomic analysis of genetic variation in European *Drosophila melanogaster*. Our analyses uncover longitudinal population structure, provide evidence for continent-wide selective sweeps, identify candidate genes for local climate adaptation, and document clines in chromosomal inversion and transposable element frequencies. We also characterise variation among populations in the composition of the fly microbiome, and identify five new DNA viruses in our samples.

Introduction

Understanding processes that influence genetic variation in natural populations is fundamental to understanding the process of evolution (Dobzhansky 1970; Lewontin 1974; Kreitman 1983; Kimura 1984; Hudson *et al.* 1987; McDonald & Kreitman 1991; Adrian & Comeron 2013). Until recently, technological constraints have limited studies of natural genetic variation to small regions of the genome and small numbers of individuals. With the development of population genomics, we can now analyse patterns of genetic variation for large numbers of individuals genome-wide, with samples structured across space and time. As a result, we have new insight into the evolutionary dynamics of genetic variation in natural populations (e.g., Hohenlohe *et al.* 2010; Cheng *et al.* 2012; Begun *et al.* 2007; Pool *et al.* 2012; Harpur *et al.* 2014; Zanini *et al.* 2015). But, despite this technological progress, extensive large-scale sampling and genome sequencing of populations remains prohibitively expensive and too labor-intensive for most individual research groups.

Here, we present the first comprehensive, continent-wide genomic analysis of genetic variation of European *Drosophila melanogaster*, based on 48 pool-sequencing samples from 32 localities collected in 2014 (fig. 1) by the European *Drosophila* Population Genomics Consortium (*DrosEU*;

https://droseu.net). *D. melanogaster* offers several advantages for genomic studies of evolution in space and time. It boasts a relatively small genome, a broad geographic range, a multivoltine life history which allows sampling across generations on short timescales, simple standard techniques for collecting wild samples, and a well-developed context for population genomic analysis (e.g., Powell 1997; Keller 2007; Hales *et al.* 2015). Importantly, this species is studied by an extensive international research community, with a long history of developing shared resources (Larracuente & Roberts 2015; Bilder & Irvine 2017; Haudry *et al*. 2020).

Our study complements and extends previous studies of genetic variation in *D. melanogaster*, both from its native range in sub-Saharan Africa and from its world-wide expansion as a human commensal. The expansion into Europe is thought to have occurred approximately 4,100 - 19,000 years ago and into North America and Australia in the last few centuries (e.g., Lachaise *et al.* 1988; David & Capy 1988; Li & Stephan 2006; Keller 2007; Sprengelmeyer *et al* 2018; Kapopoulou *et al.* 2018a; Arguello *et al.* 2019). The colonization of novel habitats and climate zones on multiple continents makes *D. melanogaster* especially useful for studying parallel local adaptation, with previous studies finding pervasive latitudinal clines in allele frequencies (e.g., Schmidt & Paaby 2008; Turner *et al.* 2008; Kolaczkowski *et al.* 2011; Fabian *et al.* 2012; Bergland *et al.* 2014; Machado *et al.* 2016; Kapun *et al.* 2016a), structural variants such as chromosomal inversions (reviewed in Kapun & Flatt 2019), transposable elements (TEs) (Boussy *et al.* 1998; González *et al.* 2008; 2010), and complex phenotypes (de Jong & Bochdanovits 2003; Schmidt & Paaby 2008; Schmidt *et al.* 2008; Kapun *et al.* 2016b; Behrman *et al.* 2018), especially along the North American and Australian east coasts. In addition to parallel local adaptation, these latitudinal clines are, however, also affected by admixture with flies from Africa and Europe (Caracristi & Schlötterer 2003; Yukilevich & True 2008a; b; Duchen *et al.* 2013; Kao *et al.* 2015; Bergland *et al.* 2016).

In contrast, the population genomics of *D. melanogaster* on the European continent remains largely unstudied (Božičević *et al.* 2016; Pool *et al.* 2016; Mateo *et al.* 2018). Because Eurasia was the first continent colonized by *D. melanogaster* as they migrated out of Africa, we sought to understand how this species has adapted to new habitats and climate zones in Europe, where it has

been established the longest (Lachaise *et al.* 1988; David & Capy 1988). We analyse our data at three levels: (1) variation at single-nucleotide polymorphisms (SNPs) in nuclear and mitochondrial (mtDNA) genomes (~5.5 x 10^6 SNPs in total); (2) structural variation, including TE insertions and chromosomal inversion polymorphisms; and (3) variation in the microbiota associated with flies, including bacteria, fungi, protists, and viruses.

Results and Discussion

As part of the *DrosEU* consortium, we collected 48 population samples of *D. melanogaster* from 32 geographical locations across Europe in 2014 (table 1; fig. 1). We performed pooled sequencing (Pool-Seq) of all 48 samples, with an average autosomal coverage ≥50x (supplementary table S1, Supplementary Material online). Of the 32 locations, 10 were sampled at least once in summer and once in fall (fig. 1), allowing a preliminary analysis of seasonal change in allele frequencies on a genome-wide scale.

A description of the basic patterns of genetic variation of these European *D. melanogaster* population samples, based on SNPs, is provided in the supplement (see supplementary results, supplementary table S1, Supplementary Material online). For each sample, we estimated genome-wide levels of π, Watterson's θ and Tajima's D (corrected for pooling; Futschik & Schlötterer 2010; Kofler *et al.* 2011). In brief, patterns of genetic variability and Tajima's D were largely consistent with what has been previously observed on other continents (e.g., Fabian *et al*. 2012; Langley *et al*. 2012; Lack *et al.* 2015, 2016), and genetic diversity across the genome varies mainly with recombination rate (Langley *et al.* 2012). We also found little spatio-temporal variation among European populations in overall levels of sequence variability (table 2).

Below we focus on the identification of selective sweeps, previously unknown longitudinal population structure across the European continent, patterns of local adaptation and clines, and microbiota.

Several genomic regions show signatures of continent-wide selective sweeps

To identify genomic regions that have likely undergone selective sweeps in European populations of *D. melanogaster*, we used *Pool-hmm* (Boitard *et al.* 2013; see supplementary table S2A, Supplementary Material online), which identifies candidate sweep regions via distortions in the allele frequency spectrum. We ran *Pool-hmm* independently for each sample and identified several genomic regions that coincide with previously identified, well-supported sweeps in the proximity of *Hen1* (Kolaczkowski *et al.* 2011), *Cyp6g1* (Daborn *et al.* 2002), *wapl* (Beisswanger *et al.* 2006), and around the chimeric gene *CR18217* (Rogers & Hartl 2012), among others (supplementary table S2B, Supplementary Material online). These regions also showed local reductions in π and Tajima's *D*, consistent with selective sweeps (fig. 2; fig. S1 and fig. S2; Supplementary Material online). The putative sweep regions that we identified in the European populations included 145 of the 232 genes previously identified using *Pool-hmm* in an Austrian population (Boitard *et al.* 2012; supplementary table S2C, Supplementary Material online). We also identified other regions which have not previously been described as targets of selective sweeps (supplementary table S2A, Supplementary Material online). Of the regions analysed, 64 showed signatures of selection across all European populations (supplementary table S2D, Supplementary Material online). Of these, 52 were located in the 10% of regions with the lowest values of Tajima's *D* (SuperExactTest; $p < 0.001$). These may represent continent-wide sweeps that predate the colonization of Europe (e.g., Beisswanger *et al.* 2006) or which have recently swept across the majority of European populations (supplementary table S2D). Interestingly, 43 of the 64 genes (67%) that showed signatures of selection across all European populations were located in regions with reduced Tajima's *D* in African populations, suggesting that selective sweeps in these genes might predate the out-of-Africa expansion (Table S2D).

We then asked if there was any indication of selective sweeps particular to a certain habitat. To this end, we classified the populations according to the Köppen-Geiger climate classification (Peel *et al.* 2007) and identified several putative sweeps exclusive to arid, temperate and cold regions (supplementary table S2A, Supplementary Material online). To shed light on potential phenotypes affected by the potential sweeps we performed a gene ontology (GO) analysis. For temperate

164 climates, this analysis showed enrichment for functions such as 'response to stimulus', 'transport',
165 and 'nervous system development'. For cold climates, it showed enrichment for 'vitamin and co-
166 factor metabolic processes' (supplementary table S2E, Supplementary Material online). There was no
167 enrichment of any GO category for sweeps associated with arid regions.

168 Thus, we identified several new candidate selective sweeps in European populations of *D.*
169 *melanogaster*, many of which occur in the majority of European populations and which merit future
170 study, using sequencing of individual flies and functional genetic experiments.

171

172 **European populations are structured along an east-west gradient**

173 We next investigated whether patterns of genetic differentiation might be due to demographic sub-
174 structuring. Overall, pairwise differentiation as measured by F_{ST} was relatively low, particularly for
175 the autosomes (autosomal F_{ST} 0.013–0.059; *X*-chromosome F_{ST}: 0.043–0.076; Mann-Whitney U test;
176 $p < 0.001$; supplementary table S1, Supplementary Material online). The *X* chromosome is expected
177 to have higher F_{ST} than the autosomes, given its relatively smaller effective population size (Mann-
178 Whitney U test; $p < 0.001$; Hutter *et al.* 2007). One population, from Sheffield (UK), was unusually
179 differentiated from the others (average pairwise $F_{ST} = 0.027$; SE= 0.00043 vs. $F_{ST} = 0.04$; SE=
180 0.00055 for comparisons without this population and with this population only; supplementary table
181 S1, Supplementary Material online). Including this sample in the analysis could potentially lead to
182 exaggerated patterns of geographic differentiation, as it is both highly differentiated and the furthest
183 west. We therefore excluded it from the following analyses of geographic differentiation, as this
184 approach is conservative. (For details see the Supplementary Material online; including or excluding
185 this population did not qualitatively change our results and their interpretation.)

186 Despite low overall levels of among-population differentiation, we found that European
187 populations exhibit clear evidence of geographic sub-structuring. For this analysis, we focused on
188 SNPs located within short introns, with a length ≤ 60 bp and which most likely reflect neutral
189 population structure (Haddrill *et al.* 2005; Singh *et al.* 2009; Parsch *et al.* 2010; Clemente & Vogl
190 2012; Lawrie *et al.* 2013). We restricted our analyses to polymorphisms in regions of high

recombination (r > 3 cM/Mb; Comeron *et al.* 2011) and to SNPs at least 1 Mb away from the breakpoints of common inversions (and excluding the inversion bodies themselves), resulting in 4,034 SNPs used for demographic analysis. Focusing on high-recombination regions is important because reduced rates of crossing over in low recombination regions might make the identification of putative targets of selection difficult (cf. Kolaczkowski *et al.* 2011; Fabian *et al.* 2012).

We found two signatures of geographic differentiation using these putatively neutral SNPs. First, we identified a weak but significant correlation between pairwise F_{ST} and geographic distance, consistent with isolation by distance (IBD; Mantel test; $p < 0.001$; R^2=0.12, max. $F_{ST} \sim 0.045$; fig. 3A). Second, a principal components analysis (PCA) on allele frequencies showed that the three most important PC axes explain >25% of the total variance (PC1: 16.71%, PC2: 5.83%, PC3: 4.6%, eigenvalues = 159.8, 55.7, and 44, respectively; fig 3B). The first axis, PC1, was strongly correlated with longitude ($F_{1,42} = 118.08$, $p < 0.001$; table 2). Again, this pattern is consistent with IBD, as the European continent extends further in longitude than latitude. We repeated the above PCA using SNPs in four-fold degenerate sites, as these are also assumed to be relatively unaffected by selection (Akashi 1995; Halligan & Keightley 2006; supplementary fig. S3, Supplementary Material online), and found highly consistent results.

Because there was a significant spatial autocorrelation between samples (as indicated by Moran's test on residuals from linear regressions with PC1; $p < 0.001$; table 2), we repeated the analysis with an explicit spatial error model; the association between PC1 and longitude remained significant. To a lesser extent PC2 was likewise correlated with longitude ($F_{1,42} = 7.15$, $p < 0.05$), but also with altitude ($F_{1,42} = 11.77$, $p < 0.01$) and latitude ($F_{1,42} = 4.69$, $p < 0.05$; table 2). Similar to PC2, PC3 was strongly correlated with altitude ($F_{1,42} = 19.91$, $p < 0.001$; table 2). We also examined these data for signatures of genetic differentiation between samples collected at different times of the year. For the dataset as a whole, no major PC axes were correlated with season, indicating that there were no strong differences in allele frequencies shared between all our summer and fall samples ($p > 0.05$ for all analyses; table 2). For the 10 locations sampled in both summer and fall, we performed separate PC analyses for summer and fall. Summer and fall values of PC1 (adjusted R^2: 0.98; $p < 0.001$), PC2 (R^2: 0.74; $p <$

218 0.001) and PC3 (R^2: 0.81; $p < 0.001$) were strongly correlated across seasons. This indicates a high
219 degree of seasonal stability in local genetic variation.

220 Next, we attempted to determine if populations could be statistically classified into clusters of
221 similar populations. Using hierarchical model fitting based on the first four PC axes from the PCA
222 mentioned above, we found two distinct clusters (fig. 3B) separated along PC1, supporting the notion
223 of strong longitudinal differentiation among European populations. Similarly, model-based spatial
224 clustering also showed that populations were separated mainly by longitude (fig. 3C; using ConStruct,
225 with K=3 spatial layers chosen based on model selection procedure via cross-validation). We also
226 inferred levels of admixture among populations from this analysis, based on the relationship between
227 F_{ST} and migration rate (Wright *et al.* 1951) and using recent estimates of N_e in European populations
228 ($N_e \sim 3.1 \times 10^6$; Duchen *et al.* 2011; for pairwise migration rates see supplementary table S3,
229 Supplementary Material online). Within the Western European cluster and between the clusters, $4N_em$
230 was similar ($4N_em$-WE = 43.76, $4N_em$-between = 45.97); in Eastern Europe, estimates of $4N_em$
231 indicate significantly higher levels of admixture, despite the larger geographic range covered by these
232 samples ($4N_em$ = 74.17; Mann Whitney U-Test; $p < 0.001$). This result suggests that the longitudinal
233 differentiation in Europe might be partly driven by high levels of genetic exchange in Eastern Europe,
234 perhaps due to migration and recolonization after harsh winters in that region. However, these
235 estimates of gene flow must be interpreted with caution, as unknown demographic events can
236 confound estimates of migration rates from F_{ST} (Whitlock & MacCauley 1999).

237 In addition to restricted gene flow between geographic areas, local adaptation may explain
238 population sub-structure, even at neutral sites, if nearby and closely related populations are
239 responding to similar selective pressures. We investigated whether any of 19 climatic variables,
240 obtained from the WorldClim database (Hijmans *et al.* 2005), were associated with the genetic
241 structure in our samples. These climatic variables represent interpolated averages across 30 years of
242 observation at the geographic coordinates corresponding to our sampling locations. Since many of
243 these variables are highly intercorrelated, we analysed their joint effects on genetic variation, by using
244 PCA to summarize the information they capture. The first three climatic PC axes capture more than

77% of the variance in the 19 climatic variables (supplementary table S4, Supplementary Material online). PC1 explained 36% of the variance and was strongly correlated (r >0.75 or r <-0.75) with climatic variables differentiating 'hot and dry' from 'cold and wet' climates (e.g., maximum temperature of the warmest month, r = 0.84; mean temperature of warmest quarter, r = 0.86; annual mean temperature, r = 0.85; precipitation during the warmest quarter, r = -0.87). Conversely, PC2 (27.3% of variance explained) distinguished climates with low and high differences between seasons (*e.g.*, isothermality, r = 0.83; temperature seasonality, r = 0.88; temperature annual range, r =-0.78; precipitation in coldest quarter, r = 0.79). PC1 was strongly correlated with latitude (linear regression: $R^2 = 0.48$, $p < 0.001$), whereas PC2 was strongly correlated with longitude ($R^2 = 0.58$, $p < 0.001$). PC2 was also correlated with latitude ($R^2 = 0.11$, $p < 0.05$) and with altitude ($R^2 = 0.12$, $p < 0.01$).

We next asked whether any of these climate PCs explained any of the genetic structure uncovered above. Pairwise linear regressions of the first three PC axes based on allele frequencies of intronic SNPs against the first three climatic PCs revealed that only one significant correlation after Bonferroni correction: between climatic PC2 ('seasonality') vs. genetic PC1 (longitude; adjusted α = 0.017; $R^2 = 0.49$, $P<0.001$). This suggests that longitudinal differentiation along the European continent might be partly driven by the transition from oceanic to continental climate, possibly leading to local adaptation to gradual changes in temperature seasonality and the severity of winter conditions.

Interestingly, the central European division into an eastern and a western clade of *D. melanogaster* closely resembles known hybrid zones of organisms which form closely related pairs of sister taxa. These biogeographic patterns have been associated with long-term reductions of gene flow between eastern and western population during the last glacial maximum, followed by postglacial recolonization of the continent from southern refugia (Hewitt 1999). However, in contrast to many of these taxa, which often exhibit pronounced pre- and postzygotic isolation (Szymura & Barton 1986; Haas & Brodin 2005; Macholán *et al.* 2008, Knief *et al.* 2019), we found low genome-wide differentiation among eastern and western populations (average max. $F_{ST} \sim 0.045$), perhaps indicating that the longitudinal division of European *D. melanogaster* is not the result of postglacial secondary

contact.

Climatic predictors identify genomic signatures of local climate adaptation

To further explore climatic patterns, and to identify signatures of local adaptation caused by climatic differences among populations independent of neutral demographic effects, we tested for associations of SNP alleles with climatic PC1 and PC2 using BayeScEnv (de Villemereuil & Gaggiotti 2015). The total number of SNPs tested and the number of "top SNPs" (q-value < 0.05) are given in supplementary table S5A (Supplementary Material online). A large proportion of the top SNPs were intergenic (PC1: 33.5%; PC2: 32.2%) or intronic variants (PC1: 50.1%; PC2: 50.5%). Manhattan plots of q-values for all SNPs are shown in fig. 4. These figures show some distinct "peaks" of highly differentiated SNPs along with some broader regions of moderately differentiated SNPs (fig. 4). For example, the circadian rhythm gene *timeout* and the ecdysone signalling genes *Eip74EF* and *Eip75B* all lie near peaks associated with climatic PC1 ('hot/dry' vs. 'cold/wet'; fig. 4, top panels). We note that the corresponding genes have been identified in previous studies of clinal (latitudinal) differentiation in North American *D. melanogaster* (Fabian *et al.* 2012; Machado *et al.* 2016). Indeed, we found a significant overlap between genes associated with PC1 and PC2 (both of which are correlated with latitude) in our study and candidate gene sets from these previous studies of latitudinal clines (SuperExactTest; $p < 0.001$; Fabian *et al.* 2012; Machado *et al.* 2016). For example, out of 1,974 latitudinally varying loci along the North American east coast identified by Fabian *et al.* (2012), we found 403 (20%) and 505 (26%) of them to also be associated with PC1 and PC2 in European populations, respectively (table S5B-C). Moreover, the BayeScEnv analysis and *Pool-hmm* analysis together identify four regions with both climatic associations and evidence for continent-wide selective sweeps (supplementary table S5B-C, Supplementary Material online). Finally, four other BayeScEnv candidate genes were previously identified as targets of selection in African and North American populations based on significant McDonald-Kreitman tests (Langley *et al.* 2012; see supplementary table S5B-C, Supplementary Material online).

We next asked whether any insights into the targets of local selection could be gleaned from

examining the functions of genes near the BayeScEnv peaks. We examined annotated features within 2kb of significantly associated SNPs (PC1: 3,545 SNPs near 2,078 annotated features; PC2: 5,572 SNPs near 2,717 annotated features; supplementary table S5B and C, Supplementary Material online). First, we performed a GO term analysis with GOwinda (Kofler & Schlötterer 2012) to ask whether SNPs associated with climatic PCs are enriched for any gene functions. For PC1, we found no GO term enrichment. For PC2, we found enrichment for "cuticle development", and "UDP-glucosyltransferase activity". Next, we performed functional annotation clustering with DAVID (v6.8; Huang *et al.* 2009), and identified 37 and 47 clusters with an enrichment score > 1.3 for PC1 and PC2, respectively (supplementary table S5D-E, Supplementary Material online, Huang et al 2009). PC1 was enriched for categories such as "sex differentiation" and "response to nicotine", whereas PC2 was enriched for functional categories such as "response to nicotine", "integral component of membrane", and "sensory perception of chemical stimulus" (supplementary table S5D-E, Supplementary Material online).

We also asked whether the SNPs identified by BayeScEnv show consistent signatures of local adaptation. Many associated genes (1,205) were also shared between PC1 and PC2. Some genes have indeed been previously implicated in climatic and clinal adaptation, such as the circadian rhythm genes *timeless*, *timeout*, and *clock*, the sexual differentiation gene *fruitless*, and the *couch potato* locus which underlies the latitudinal cline in reproductive dormancy in North America (e.g., Tauber *et al.* 2007; Schmidt *et al.* 2008; Fabian *et al.* 2012). Notably, these also include the major insulin signaling genes *insulin-like receptor* (*InR)* and *forkhead box subgroup O* (*foxo*), which have strong genomic and experimental evidence implicating these loci in clinal, climatic adaptation along the North America east coast (Paaby *et al.* 2010; Fabian *et al.* 2012; Paaby *et al.* 2014; Durmaz *et al.* 2019). Thus, European populations share multiple potential candidate targets of selection with North American populations (cf. Fabian *et al.* 2012; Machado *et al.* 2016; also see Božičević *et al.* 2016). We next turned to examining polymorphisms other than SNPs, i.e. mitochondrial haplotypes as well as inversion and TE polymorphisms.

Mitochondrial haplotypes also exhibit longitudinal population structure

Mitochondrial haplotypes also showed evidence of longitudinal demographic structure in European population. We identified two main alternative mitochondrial haplotypes in Europe, G1 and G2, each with several sub-haplotypes (G1.1 and G1.2 and G2.1, G2.2 and G2.3). The two sub-types, G1.2 and G2.1, are separated by 41 mutations (fig. 5A). The frequencies of the alternative G1 and G2 haplotype varied among populations between 35.1% and 95.6% and between 4.4% and 64.9%, respectively (fig. 5B). Qualitatively, three types of European populations could be distinguished based on these haplotypes: (1) central European populations, with a high frequency (> 60%) of G1 haplotypes, (2) Eastern European populations in summer, with a low frequency (< 40%) of G1 haplotypes, and (3) Iberian and Eastern European populations in fall, with a frequency of G1 haplotypes between 40-60% (supplementary fig. S4, Supplementary Material online). Analyses of mitochondrial haplotypes from a North American population (Cooper *et al.* 2015) as well as from worldwide samples (Wolff *et al.* 2016) also revealed high levels of haplotype diversity.

While there was no correlation between the frequency of G1 haplotypes and latitude, G1 haplotypes and longitude were weakly but significantly correlated ($r^2 = 0.10$; $p < 0.05$). We thus divided the dataset into an eastern and a western sub-set along the 20º meridian, corresponding to the division of two major climatic zones, temperate (oceanic) versus cold (continental) (Peel *et al.* 2007). This split revealed a clear correlation ($r^2=0.5$; $p<0.001$) between longitude and the frequency of G1 haplotypes, explaining as much as 50% of the variation in the western group (supplementary fig. S4B, Supplementary Material online). Similarly, in eastern populations, longitude and the frequency of G1 haplotypes were correlated ($r^2 = 0.2$; $p<0.001$), explaining approximately 20% of the variance (supplementary fig. S4B, Supplementary Material online). Thus, these mitochondrial haplotypes appear to follow a similar east-west population structure as observed for the nuclear SNPs described above.

The frequency of polymorphic TEs varies with longitude and altitude

To examine the population genomics of structural variants, we first focused on transposable elements

353 (TEs). Similar to previous findings, the repetitive content of the 48 samples ranged from 16% to 21%
354 of the nuclear genome size (Quesneville *et al.* 2005; fig. 6). The vast majority of detected repeats
355 were TEs, mostly long terminal repeat elements (LTRs; range 7.55 % - 10.15 %) and long
356 interspersed nuclear elements (LINEs range 4.18 % - 5.52 %), along with a few DNA elements (range
357 1.16 % - 1.65 %) (supplementary table S6, Supplementary Material online). LTRs have been
358 previously described as being the most abundant TEs in the *D. melanogaster* genome (Kaminker *et al.*
359 2002; Bergman *et al.* 2006). Correspondingly, variation in the proportion of LTRs best explained
360 variation in total TE content (LINE+LTR+DNA) (Pearson's $r = 0.87$, $p < 0.01$, *vs.* DNA $r = 0.58$, $p =$
361 0.0117, and LINE $r = 0.36$, $p < 0.01$ and supplementary fig. S5A, Supplementary Material online).

362 For each of the 1,630 TE insertion sites annotated in the *D. melanogaster* reference genome *v.6.04*,
363 we estimated the frequency at which a copy of the TE was present at that site using *T-lex2* (Fiston-
364 Lavier *et al.* 2015; see supplementary table S7, Supplementary Material online). On average, 56%
365 were fixed in all samples. The remaining polymorphic TEs mostly segregated at low frequency in all
366 samples (supplementary fig. S5B), potentially due to purifying selection (González *et al.* 2008; Petrov
367 *et al.* 2011; Kofler *et al.* 2012; Cridland *et al.* 2013; Blumenstiel *et al.* 2014). However, 246 were
368 present at intermediate frequencies (>10% and <95%) and located in regions of non-zero
369 recombination (Fiston-Lavier *et al.* 2010; Comeron *et al.* 2012; see supplementary table S7,
370 Supplementary Material online). Although some of these insertions might be segregating neutrally at
371 transposition-selection balance (Charlesworth *et al.* 1994; see supplementary fig. S5B, Supplementary
372 Material online), they are likely enriched for candidate adaptive mutations (Rech *et al.* 2019).

373 In each of the 48 samples, TE frequency and recombination rate were negatively correlated
374 genome-wide (Spearman rank sum test; $p < 0.01$), as has also been previously reported for *D.*
375 *melanogaster* (Bartolomé *et al.* 2002; Petrov *et al.* 2011; Kofler *et al.* 2012). This remains true when
376 fixed TE insertions were excluded (population frequency ≥95%) from the analysis, although it was
377 not statistically significant for some chromosomes and populations (supplementary table S8,
378 Supplementary Material online). In both cases, the correlation was stronger when broad-scale (Fiston-
379 Lavier *et al.* 2010) rather than fine-scale (Comeron *et al.* 2012) recombination rate estimates were

used, indicating that the former may best capture long-term population recombination patterns (see supplementary materials and methods and supplementary table S8, Supplementary Material online).

We next tested whether variation in TE frequencies among samples was associated with spatially or temporally varying factors. We focused on 111 TE insertions that segregated at intermediate frequencies, were located in non-zero recombination regions, and that showed an interquartile range (IQR) > 10 (see supplementary materials and methods, Supplementary Material online). Of these insertions, 57 were significantly associated with a at least one variable of interest after multiple testing correction (supplementary table S9A, Supplementary Material online): 13 were significantly associated with longitude, 13 with altitude, five with latitude, three with season, and 23 insertions with more than one of these variables (supplementary table S9A, Supplementary Material online). These 57 TEs were mainly located inside genes (42 out of 57; Fisher's Exact Test, $p > 0.05$; supplementary table S9A, Supplementary Material online).

The 57 TEs significantly associated with these environmental variables were enriched for two TE families: the LTR *297* family with 11 copies, and the DNA *pogo* family with five copies (χ^2-values after Yate's correction < 0.05; supplementary table S9B, Supplementary Material online). Interestingly, 17 of the 57 TEs coincided with previously identified adaptive candidate TEs, suggesting that our dataset might be enriched for adaptive insertions (SuperExactTest, $p < 0.001$), several of which exhibit spatial frequency clines that deviate from neutral expectation (SuperExactTest, $p < 0.001$, supplementary table S9A, Supplementary Material online; cf.; Rech *et al*. 2019). Moreover, 18 of the 57 TEs also show significant correlations with either geographical or temporal variables in North American populations (SuperExactTest, $p < 0.001$, supplementary table S9A, Supplementary Material online; cf.; Lerat *et al.* 2019).

Inversions exhibit latitudinal and longitudinal clines in Europe

Polymorphic chromosomal inversions, another class of structural variants besides TEs, are well-known to exhibit pronounced spatial (clinal) patterns in North American, Australian and other populations, possibly due to spatially varying selection (reviewed in Kapun & Flatt 2019; also see

Mettler *et al.* 1977; Knibb *et al.* 1981; Leumeunier & Aulard 1992; Hoffmann & Weeks 2007; Fabian *et al.* 2012; Kapun *et al.* 2014; Rane *et al.* 2015; Adrion *et al.* 2015; Kapun *et al.* 2016a). However, in contrast to North America and Australia, inversion clines in Europe remain very poorly characterized (Lemeunier & Aulard 1992; Kapun & Flatt 2019). We therefore sought to examine the presence and frequency of six cosmopolitan inversions (*In(2L)t, In(2R)NS, In(3L)P, In(3R)C, In(3R)Mo, In(3R)Payne*) in our European samples, using a panel of highly diagnostic inversion-specific marker SNPs, identified through sequencing of cytologically determined karyotypes by Kapun *et al.* (2014) (also see Kapun *et al.* 2016a). All 48 samples were polymorphic for one or more inversions (Figure 6). However, only *In(2L)t* segregated at substantial frequencies in most populations (average frequency = 20.2%); all other inversions were either absent or rare (average frequencies: *In(2R)NS* = 6.2%, *In(3L)P* = 4%, *In(3R)C* = 3.1%, *In(3R)Mo* =2.2%, *In(3R)Payne* = 5.7%) (cf. Kapun *et al.* 2016a; Kapun & Flatt 2019).

Despite their overall low frequencies, several inversions showed pronounced clinality, in qualitative agreement with findings from other continents (Lemeunier & Aulard 1992; Kapun & Flatt 2019). For the analyses below, we tested for potentially confounding effects of significant residual spatial autocorrelation among samples; all of these test were negative, except for *In(3R)C* (Moran's $I \approx 0$, $p > 0.05$ for all tests; table 3). We observed significant latitudinal clines in Europe for *In(3L)P, In(3R)C* and *In(3R)Payne* (binomial generalized linear model: Inversion frequency ~ Latitude + Longitude + Altitude + Season; effect of Latitude: $p < 0.001$ for all; see table 3). Clines for *In(3L)P* and *In(3R)Payne* were similar between Europe and North America (with frequencies for both decreasing with latitude, $p < 0.05$; see supplementary table S10, Supplementary Material online). However, all inversions differed in their frequency at the same latitude between North America and Europe ($p < 0.001$ for the Latitude × Continent interaction; supplementary table S10, Supplementary Material online).

Latitudinal inversion clines previously observed along the North American and Australian east coasts (supplementary fig. S6 and supplementary table S10, Supplementary Material online; Kapun *et al.* 2016a) have been attributed to spatially varying selection, especially in the case of *In(3R)Payne*

(Durmaz *et al.* 2018; Anderson *et al.* 2005; Umina *et al.* 2005; Kennington *et al.* 2006; Rako *et al.* 2006; Kapun *et al.* 2016a,b; Kapun & Flatt 2019). Similar to patterns in North America (Kapun *et al.* 2016a), we observed that clinality of the three inversion polymorphisms was markedly stronger than for putatively neutral SNPs in short introns (see supplementary table S11, Supplementary Material online), suggesting that these polymorphisms are maintained non-neutrally. Together, these findings suggest that latitudinal inversion clines in Europe are shaped by spatially varying selection, as they are in North America (Kapun *et al.* 2016a; Kapun & Flatt 2019).

We also detected longitudinal clines for *In(2L)t* and *In(2R)NS*, with both polymorphisms decreasing in frequency from east to west (see table 3; $p < 0.01$; also cf. Kapun & Flatt 2019). Longitudinal clines for these two inversions have also been found in North America (cf. Kapun & Flatt 2019). One of these inversions, *In(2L)t*, also changed in frequency with altitude (table 3; $p < 0.001$). These longitudinal and altitudinal inversion clines did, however, not deviate from neutral expectation (supplementary table S11, Supplementary Material online).

European *Drosophila* microbiomes contain Entomophthora, trypanosomatids and previously unknown DNA viruses

The microbiota can affect life history traits, immunity, hormonal physiology, and metabolic homeostasis of their fly hosts (e.g., Trinder *et al.* 2017; Martino *et al.* 2017) and might thus reveal interesting patterns of local adaptation. We therefore examined the bacterial, fungal, protist, and viral microbiota sequence content of our samples. To do this, we characterised the taxonomic origin of the non-*Drosophila* reads in our dataset using MGRAST, which identifies and counts short protein motifs ('features') within reads (Meyer *et al.* 2008). We examined 262 million reads in total. Of these, most were assigned to *Wolbachia* (mean 53.7%; fig. 7; supplementary table S1), a well-known endosymbiont of *Drosophila* (Werren *et al.* 2008). The abundance of *Wolbachia* protein features relative to other microbial protein features (relative abundance) varied strongly between samples, ranging from 8.8% in a sample from Ukraine to almost 100% in samples from Spain, Portugal, Turkey and Russia (supplementary table S12, Supplementary Material online). Similarly, *Wolbachia*

loads varied 100-fold between samples, as estimated from the ratio of *Wolbachia* protein features to *Drosophila* protein features (supplementary table S12, Supplementary Material online). In contrast to a previous study (Kriesner *et al*. 2016), there was no evidence for clinality of *Wolbachia* loads (p = 0.13, longitude; p = 0.41, latitude; Kendall's rank correlation). However, these authors measured infection frequencies while we measured *Wolbachia* loads in pooled samples. Because the frequency of infection does not necessarily correlate with microbial loads measured in pooled samples, we might not have been able to detect such a signal in our data.

Acetic acid bacteria of the genera *Gluconobacter*, *Gluconacetobacter*, and *Acetobacter* were the second largest group, with an average relative abundance of 34.4% among microbial protein features. Furthermore, we found evidence for the presence of several genera of Enterobacteria (*Serratia, Yersinia, Klebsiella, Pantoea, Escherichia, Enterobacter, Salmonella*, and *Pectobacterium*). *Serratia* occurs only at low frequencies or is absent from most of our samples, but reaches a very high relative abundance among microbial protein features in the Nicosia (Cyprus) summer collection (54.5%). This high relative abundance was accompanied by an 80x increase in *Serratia* bacterial load.

We also detected several eukaryotic microorganisms, although they were less abundant than the bacteria. We found trypanosomatids, previously reported to be associated with *Drosophila* in other studies (Wilfert *et al.* 2011; Chandler & James 2013; Hamilton *et al.* 2015), in 16 of our samples, on average representing 15% of all microbial protein features identified in these samples.

Fungal protein features make up <3% of all but three samples (from Finland, Austria and Turkey; supplementary table S12, Supplementary Material online). This is somewhat surprising because yeasts are commonly found on rotting fruit, the main food substrate of *D. melanogaster*, and co-occur with flies (Barata *et al.* 2012; Chandler *et al.* 2012). This result suggests that, although yeasts can attract flies and play a role in food choice (Becher *et al.* 2012; Buser *et al.* 2014), they might not be highly prevalent in or on *D. melanogaster* bodies. One reason might be that they are actively digested and thus not part of the microbiome. We also found the fungal pathogen *Entomophthora muscae* in 14 samples, making up 0.18% of the reads (Elya *et al.* 2018).

Our data also allowed us to identify DNA viruses. Only one DNA virus has been previously

488 described for *D. melanogaster* (Kallithea virus; Webster *et al.* 2015; Palmer *et al.* 2018) and only two
489 additional ones from other Drosophilid species (*Drosophila innubila* Nudivirus [Unckless 2011],
490 Invertebrate Iridovirus 31 in *D. obscura* and *D. immigrans* [Webster *et al.* 2016]). In our data set,
491 approximately two million reads came from *Kallithea* nudivirus (Webster *et al.* 2015), allowing us to
492 assemble the first complete *Kallithea* genome (>300-fold coverage in the Ukrainian sample
493 UA_Kha_14_46; Genbank accession KX130344).

494 We also found reads from five additional DNA viruses that were previously unknown
495 (supplementary table S13, Supplementary Material online). First, around 1,000 reads come from a
496 novel nudivirus closely related to both *Kallithea* virus and to *Drosophila innubila* nudivirus (Unckless
497 2011) in sample DK_Kar_14_41 from Karensminde, Denmark supplementary table S13,
498 Supplementary Material online). As the reads from this virus were insufficient to assemble the
499 genome, we identified a publicly available dataset (SRR3939042: 27 male *D. melanogaster* from
500 Esparto, California; Machado *et al.* 2016) with sufficient reads to complete the genome (provisionally
501 named "*Esparto* Virus"; KY608910). Second, we also identified two novel Densoviruses
502 (*Parvoviridae*). The first is a relative of *Culex pipiens* densovirus, provisionally named "*Viltain*
503 virus", found at 94-fold coverage in sample FR_Vil_14_07 (Viltain; KX648535). The second is
504 "*Linvill Road* virus", a relative of *Dendrolimus punctatus* densovirus, represented by only 300 reads
505 here, but with high coverage in dataset SRR2396966 from a North American sample of *D. simulans*,
506 permitting assembly (KX648536; Machado *et al.* 2016). Third, we detected a novel member of the
507 *Bidnaviridae* family, "*Vesanto* virus", a bidensovirus related to *Bombyx mori* densovirus 3 with
508 approximately 900-fold coverage in sample FI_Ves_14_38 (Vesanto; KX648533 and KX648534).
509 Finally, in one sample (UA_Yal_14_16), we detected a substantial number of reads from an
510 Entomopox-like virus, which we were unable to fully assemble (supplementary table S13,
511 Supplementary Material online).

512 Using a detection threshold of >0.1% of the *Drosophila* genome copy number, the most commonly
513 detected viruses were *Kallithea* virus (30/48 of the pools) and *Vesanto* virus (25/48), followed by
514 *Linvill Road* virus (7/48) and *Viltain* virus (5/48), with *Esparto* virus and the entomopox-like virus

being the rarest (2/48 and 1/48, respectively). Because *Wolbachia* can protect *Drosophila* from viruses (Teixeira et al., 2008), we hypothesized that *Wolbachia* loads might correlate negatively with viral loads, but found no evidence of such a correlation ($p = 0.83$ Kallithea virus; $p = 0.76$ Esparto virus; $p = 0.52$ Viltain virus; $p = 0.96$ Vesanto 1 virus; $p = 0.93$ Vesanto 2 virus; $p = 0.5$ Linvill Road virus; Kendall's rank correlation). Perhaps this is because the *Kallithea* virus, the most prevalent virus in our data set, is not expected to be affected by *Wolbachia* (Palmer et al.,2018). Similarly, Shi et al. (2018) found no link between *Wolbachia* and the prevalence or abundance of RNA viruses in data from individual flies.

The variation in bacterial microbiomes across space and time reported here is analysed in more detail in Wang *et al.* (2020); this study suggests that some of this variation is structured geographically (cf. Walters *et al.* 2020). Thus, microbiome composition might contribute to phenotypic differences and local adaptation among populations (Haselkorn *et al.* 2009; Richardson *et al.* 2012; Staubach *et al.* 2013; Kriesner *et al.* 2016; Wang and Staubach 2018).

Conclusions

Here, we have comprehensively sampled and sequenced European populations of *D. melanogaster* for the first time (fig. 1). We find that European *D. melanogaster* populations are longitudinally differentiated for putatively neutral SNPs, mitochondrial haplotypes as well as for inversion and TE insertion polymorphisms. Potentially adaptive polymorphisms also show this pattern, possibly driven by the transition from oceanic to continental climate along the longitudinal axis of Europe. We note that this longitudinal differentiation qualitatively resembles the one observed for human populations in Europe (e.g., Cavalli-Sforza 1966; Xiao et al. 2004; Francalacci & Sanna 2008; Novembre *et al.* 2008). Given that *D. melanogaster* is a human commensal (Keller 2007, Arguello *et al.* 2019), it is thus tempting to speculate that the demographic history of European populations might have been influenced by past human migration. Outside Europe, east-west structure has been previously found in sub-Saharan Africa populations of *D. melanogaster*, with the split between eastern and western African populations having occurred ~70 kya (Michalakis & Veuille 1996; Aulard *et al.* 2002;

542 Kapopoulou *et al.* 2018b), a period that coincides with a wave of human migration from eastern into
543 western Africa (Nielsen *et al.* 2017). However, in contrast to the pronounced pattern observed in
544 Europe, African east-west structure is relatively weak, explaining only ~2.7% of variation, and is
545 primarily due to an inversion whose frequency varies longitudinally. In contrast, our demographic
546 analyses are based on SNPs located in >1 Mb distance from the breakpoints of the most common
547 inversions and excluding the inversion bodies, making it unlikely that the longitudinal pattern we
548 observe is driven by inversions.

549 Our extensive sampling was feasible only due to synergistic collaboration among many research
550 groups. Our efforts in Europe are paralleled in North America by the *Dros-RTEC* consortium
551 (Machado *et al.* 2019), with whom we are collaborating to compare population genomic data across
552 continents. Together, we have sampled both continents annually since 2014; we aim to continue to
553 sample and sequence European and North American *Drosophila* populations with increasing spatio-
554 temporal resolution in future years. With these efforts, we hope to provide a rich community resource
555 for biologists interested in molecular population genetics and adaptation genomics.

556

557 **Materials and methods**

558 A detailed description of the materials and methods is provided in the supplementary materials and
559 methods (see Supplementary Material online); here we give a brief overview of the dataset and the
560 basic methods used. The 2014 *DrosEU* dataset represents the most comprehensive spatio-temporal
561 sampling of European *D. melanogaster* populations to date (fig.1; supplementary table S1,
562 Supplementary Material online). It comprises 48 samples of *D. melanogaster* collected from 32
563 geographical locations across Europe at different time points in 2014 through a joint effort of 18
564 research groups. Collections were mostly performed with baited traps using a standardized protocol
565 (see supplementary materials and methods, Supplementary Material online). From each collection, we
566 pooled 33–40 wild-caught males. We used males as they are more easily distinguishable
567 morphologically from similar species than females. Despite our precautions, we identified a low level
568 of *D. simulans* contamination in our sequences; we computationally filtered these sequences from the

data prior to further analysis (see Supplementary Material online). To sequence these samples, we extracted DNA and barcoded each sample, and sequenced the ~40 flies per sample as a pool (Pool-Seq; Schlötterer *et al.* 2014), as paired-end fragments on a *Illumina NextSeq 500* sequencer at the Genomics Core Facility of Pompeu Fabra University. Samples were multiplexed in 5 batches of 10 samples, except for one batch of 8 samples (supplementary table S1, Supplementary Material online). Each multiplexed batch was sequenced on 4 lanes at ~50x raw coverage per sample. The read length was 151 bp, with a median insert size of 348 bp (range 209-454 bp). Our genomic dataset is available under NCBI Bioproject accession PRJNA388788. Sequences were processed and mapped to the *D. melanogaster* reference genome (v.6.12) and reference sequences from common commensals and pathogens. Our bioinformatic pipeline is available at https://github.com/capoony/DrosEU_pipeline. To call SNPs, we developed custom software (*PoolSNP*; see supplementary material and methods; https://github.com/capoony/PoolSNP), using stringent heuristic parameters. In addition, we obtained genome sequences from African flies from the *Drosophila* Genome Nexus (DGN; http://www.johnpool.net/genomes.html; see supplementary table S14 for SRA accession numbers). We used data from 14 individuals from Rwanda and 40 from Siavonga (Zambia). We mapped these data to the *D. melanogaster* reference genome using the same pipeline as for our own data above, and built consensus sequences for each haploid sample by only considering alleles with > 0.9 allele frequencies. We converted consensus sequences to *VCF* and used *VCFtools* (Danecek et al. 2011) for downstream analyses. Additional steps in the mapping and variant calling pipeline and further downstream analyses of the data are detailed in the supplementary materials and methods (Supplementary Materials online).

Supplementary Materials

Supplementary materials and methods, supplementary results and supplementary figs. S1–S13 and supplementary tables S1–S18 are available at Molecular Biology and Evolution online (http://www.mbe.oxfordjournals.org/).

Acknowledgments

We thank three anonymous reviewers and the editors for their helpful comments on a previous version of our manuscript. We are grateful to the members of the *DrosEU* and Dros-RTEC consortia and to Dmitri Petrov (Stanford University) for support and discussion. *DrosEU* is funded by a Special Topic Networks (STN) grant from the European Society for Evolutionary Biology (ESEB). Computational analyses were partially executed at the Vital-IT bioinformatics facility of the University of Lausanne (Switzerland), the computing facilities of the CC LBBE/PRABI in Lyon (France), the bwUniCluster of the state of Baden-Württemberg (bwHPC), and the University of St Andrews Bioinformatics Unit which is funded by a Wellcome Trust ISSF award (grant 105621/Z/14/Z). We are also grateful to Simon Boitard and Oscar Gaggiotti for their helpful technical advice on *Pool-hmm* and BayeScEnv analyses, respectively.

Funding

Funder	Grant reference number	Author
University of Freiburg Research Innovation Fund 2014. Deutsche Forschungsgemeinschaft (DFG)	STA1154/4-1Project 408908608	Fabian Staubach
Academy of Finland	#268241	Maaria Kankare
Academy of Finland	#272927	Maaria Kankare
Russian Foundation of Basic Research	#15-54-46009 CT_a	Elena G. Pasyukova
Danish Natural Science Research Council	4002-00113	Volker Loeschcke
Ministerio de Economia y Competitividad	CTM2017-88080 (AEI/FEDER, UE)	Marta Pascual
CNRS	UMR 9191	Catherine Montchamp-Moreau
Vetenskapsrådet	2011-05679	Jessica Abbott
Vetenskapsrådet	2015-04680	Jessica Abbott
Emmy Noether Programme of the Deutsche Forschungsgemeinschaft,(DFG)	PO 1648/3-1	Nico Posnien
National Institute of Health (NIH)	R35GM119686	Alan O. Bergland
Ministerio de Economia y Competitividad	CGL2013-42432-P	Maria Pilar Garcia Guerreiro

Scientific and Technological Research Council of Turkey (TUBITAK)	#214Z238	Banu Sebnem Onder
ANR Exhyb	14-CE19-0016	Cristina Vieira
Network of Excellence LifeSpan	FP6 036894	Bas J. Zwaan
IDEAL	FP7/2007-2011/259679	Bas J. Zwaan
Israel Science Foundation	1737/17	Eran Tauber
National Institute of Health (NIH)	R01GM100366	Paul S. Schmidt
Deutsche Forschungsgemeinschaft (DFG)	PA 903/8-1	John Parsch
Austrian Science Fund (FWF)	P32275	Martin Kapun
Austrian Science Fund (FWF)	P27048	Andrea J. Betancourt
Biotechnology and Biological Sciences Research Council (BBSRC)	BB/P00685X/1	Andrea J. Betancourt
Swiss National Science Foundation (SNSF)	PP00P3_133641	Thomas Flatt
Swiss National Science Foundation (SNSF)	PP00P3_165836	Thomas Flatt
Swiss National Science Foundation (SNSF)	31003A_182262	Thomas Flatt
European Commission	H2020-ERC-2014CoG-647900	Josefa González
Secretaria d'Universitats i Recerca. Dept Economia i Coneixement. Generalitat de Catalunya	GRC 2017 SGR 880	Josefa González
Ministerio de Economia y Competitividad	FEDER BFU2014-57779-P	Josefa González

References

Adrian AB, Comeron JM (2013) The *Drosophila* early ovarian transcriptome provides insight to the molecular causes of recombination rate variation across genomes. *BMC Genomics*, **14**, 1-12.

Adrion JR, Hahn MW, Cooper BS (2015) Revisiting classic clines in *Drosophila melanogaster* in the age of genomics. *Trends in Genetics*, **31**, 434–444.

Akashi H (1995) Inferring weak selection from patterns of polymorphism and divergence at "silent" sites in *Drosophila* DNA. *Genetics*, **139**, 1067-1076.

Anderson AR, Hoffmann AA, McKechnie SW, Umina PA, Weeks AR (2005) The latitudinal cline in the *In(3R)Payne* inversion polymorphism has shifted in the last 20 years in Australian *Drosophila melanogaster* populations. *Molecular Ecology,* **14**, 851–858.

Arguello JR, Laurent S, Clark AG. (2019) Demographic History of the Human Commensal *Drosophila melanogaster*. *Genome Biology and Evolution* **11**:844–854.

Aulard S, David JR, Lemeunier F (2002) Chromosomal inversion polymorphism in Afrotropical populations of *Drosophila melanogaster*. *Genetic Research*, **79**, 49–63.

Barata A, Santos SC, Malfeito-Ferreira M, Loureiro V (2012) New insights into the ecological interaction between grape berry microorganisms and *Drosophila* flies during the development of sour rot. *Microbial Ecology*, **64**, 416–430.

Bartolomé C, Maside X, Charlesworth B (2002) On the Abundance and Distribution of Transposable Elements in the Genome of *Drosophila melanogaster*. *Molecular Biology and Evolution*, **19**, 926–937.

Becher PG, Flick G, Rozpędowska E *et al.* (2012) Yeast, not fruit volatiles mediate *Drosophila melanogaster* attraction, oviposition and development. *Functional Ecology*, **26**, 822–828.

Begun DJ, Holloway AK, Stevens K *et al.* (2007) Population Genomics: Whole-Genome Analysis of Polymorphism and Divergence in *Drosophila simulans*. *PLoS Biology*, **5**, e310.

Behrman EL, Howick VM, Kapun M *et al.* (2018) Rapid seasonal evolution in innate immunity of wild *Drosophila melanogaster*. *Proceedings of the Royal Society of London B*, **285**, 20172599.

Beisswanger S, Stephan W, De Lorenzo D (2006) Evidence for a Selective Sweep in the *wapl* Region of *Drosophila melanogaster*. *Genetics*, **172**, 265–274.

Bergland AO, Behrman EL, O'Brien KR, Schmidt PS, Petrov DA (2014) Genomic Evidence of Rapid and STable Adaptive Oscillations over Seasonal Time Scales in *Drosophila*. *PLoS Genetics*, **10**, e1004775.

Bergland AO, Tobler R, González J, Schmidt P, Petrov D (2016) Secondary contact and local adaptation contribute to genome-wide patterns of clinal variation in *Drosophila* melanogaster. *Molecular Ecology*, **25**, 1157–1174.

Bergman, C. M., Quesneville, H., Anxolabehere, D. & Ashburner, M. (2006) Recurrent insertion and duplication generate networks of transposable element sequences in the Drosophila melanogaster genome. *Genome Biology*, **7**, R112.

Blumenstiel JP, Chen X, He M, Bergman CM (2014) An Age-of-Allele Test of Neutrality for Transposable Element Insertions. *Genetics*, **196**, 523–538.

Boitard S, Schlötterer C, Nolte V, Pandey RV, Futschik A (2012) Detecting Selective Sweeps from Pooled Next-Generation Sequencing Samples. *Molecular Biology and Evolution*, **29**, 2177–2186.

Boitard S, Kofler R, Françoise P, Robelin D, Schlötterer C, Futschik A (2013) Pool-hmm: a Python program for estimating the allele frequency spectrum and detecting selective sweeps from next generation sequencing of pooled samples. *Mol Ecol Resour,* **13**, 337–340.

Boussy IA, Itoh M, Rand D, Woodruff RC (1998) Origin and decay of the P element-associated latitudinal cline in Australian *Drosophila melanogaster*. *Genetica*, **104**, 45–57.

Božičević V, Hutter S, Stephan W, Wollstein A (2016) Population genetic evidence for cold adaptation in European *Drosophila melanogaster* populations. *Molecular Ecology*, **25**, 1175–1191.

Buser CC, Newcomb RD, Gaskett AC, Goddard MR (2014) Niche construction initiates the evolution of mutualistic interactions. *Ecology Letters*, **17**, 1257–1264.

Caracristi G, Schlötterer C (2003) Genetic Differentiation Between American and European *Drosophila melanogaster* Populations Could Be Attributed to Admixture of African Alleles. *Molecular Biology and Evolution*, **20**, 792–799.

Cavalli-Sforza LL (1966) Population Structure and Human Evolution. *Proceedings of the Royal Society of London B*, **164**, 362–379.

Chandler JA, James PM (2013) Discovery of trypanosomatid parasites in globally distributed *Drosophila* species. *PLoS ONE*, **8**, e61937.

Chandler JA, Eisen JA, Kopp A (2012) Yeast communities of diverse *Drosophila* species: comparison of two symbiont groups in the same hosts. *Applied and Environmental Microbiology*, **78**, 7327–7336.

Charlesworth B, Sniegowski P, Stephan W (1994) The evolutionary dynamics of repetitive DNA in eukaryotes. *Nature*, **371**, 215–220.

Cheng C, White BJ, Kamdem C *et al.* (2012) Ecological genomics of *Anopheles gambiae* along a latitudinal cline: a population-resequencing approach. *Genetics*, **190**, 1417–1432.

676 Clemente F, Vogl C (2012) Unconstrained evolution in short introns? – An analysis of genome-wide
677 polymorphism and divergence data from *Drosophila*. *Journal of Evolutionary Biology*, **25**, 1975–
678 1990.
679 Cooper BS, Burrus CR, Ji C, Hahn MW, Montooth KL (2015) Similar Efficacies of Selection Shape
680 Mitochondrial and Nuclear Genes in Both *Drosophila melanogaster* and *Homo sapiens*. *G3*, **5**,
681 2165–2176.
682 Cridland JM, Macdonald SJ, Long AD, Thornton KR (2013) Abundance and distribution of
683 transposable elements in two *Drosophila* QTL mapping resources. *Molecular Biology and*
684 *Evolution*, **30**, 2311–2327.
685 Daborn PJ, Yen JL, Bogwitz MR *et al.* (2002) A single p450 allele associated with insecticide
686 resistance in *Drosophila*. *Science*, **297**, 2253–2256.
687 David JR, Capy P (1988) Genetic variation of *Drosophila melanogaster* natural populations. *Trends*
688 *in Genetics*, **4**, 106–111.
689 de Jong G, Bochdanovits Z (2003) Latitudinal clines in *Drosophila melanogaster*: body size,
690 allozyme frequencies, inversion frequencies, and the insulin-signalling pathway. *Journal of*
691 *Genetics*, **82**, 207–223.
692 Dobzhansky T (1970) *Genetics of the Evolutionary Process*. Columbia University Press.
693 Duchen P, Zivkovic D, Hutter S, Stephan W, Laurent S (2013) Demographic inference reveals
694 African and European admixture in the North American *Drosophila melanogaster* population.
695 *Genetics*, **193**, 291–301.
696 Durmaz E, Benson C, Kapun M, Schmidt P, Flatt T (2018) An Inversion Supergene in *Drosophila*
697 Underpins Latitudinal Clines in Survival Traits. *Journal of Evolutionary Biology,* **31**, 1354-1364..
698 Durmaz E, Rajpurohit S, Betancourt N, Fabian DK, Kapun M, Schmidt P, Flatt T (2019) A clinal
699 polymorphism in the insulin signaling transcription factor *foxo* contributes to life-history
700 adaptation in *Drosophila*. *Evolution,* **73**, 1774-1792.
701 Elya C, Lok TC, Spencer QE, McCausland H, Martinez CC, Eisen MB (2018) Robust manipulation
702 of the behavior of *Drosophila melanogaster* by a fungal pathogen in the laboratory, *eLife, 7,*
703 e34414

704 Fabian DK, Kapun M, Nolte V *et al.* (2012) Genome-wide patterns of latitudinal differentiation
705 among populations of *Drosophila melanogaster* from North America. *Molecular Ecology*, **21**,
706 4748–4769.
707 Fiston-Lavier A-S, Barrón MG, Petrov DA, González J (2015) T-lex2: genotyping, frequency
708 estimation and re-annotation of transposable elements using single or pooled next-generation
709 sequencing data. *Nucleic Acids Research*, **43**, e22–e22.
710 Fiston-Lavier A-S, Singh ND, Lipatov M, Petrov DA (2010) *Drosophila melanogaster* recombination
711 rate calculator. *Gene*, **463**, 18–20.
712 Francalacci P, Sanna D (2008) History and geography of human Y-chromosome in Europe: a SNP
713 perspective. *Journal of Anthropological Sciences*, **86**, 59–89.
714 Futschik A & Schlötterer C (2010) The next generation of molecular markers from massively parallel
715 sequencing of pooled DNA samples. *Genetics*, **186**, 207–218.
716 González J, Karasov TL, Messer PW, Petrov DA (2010) Genome-Wide Patterns of Adaptation to
717 Temperate Environments Associated with Transposable Elements in *Drosophila*. *PLoS Genetics*,
718 **6**, e1000905.
719 González J, Lenkov K, Lipatov M, Macpherson JM, Petrov DA (2008) High Rate of Recent
720 Transposable Element–Induced Adaptation in *Drosophila melanogaster*. *PLoS Biology*, **6**, e251.
721 Haas F, Brodin A. (2005). The Crow *Corvus corone* hybrid zone in southern Denmark and northern
722 Germany. *Ibis* **147**:649–656.
723 Haddrill PR, Charlesworth B, Halligan DL, Andolfatto P (2005) Patterns of intron sequence
724 evolution in *Drosophila* are dependent upon length and GC content. *Genome Biology*, **6**, R67.
725 Hales KG, Korey CA, Larracuente AM, Roberts DM (2015) Genetics on the Fly: A Primer on the
726 *Drosophila* Model System. *Genetics*, **201**, 815–842.
727 Halligan DL, Keightley PD 2006 Ubiquitous selective constraints in the *Drosophila* genome revealed
728 by a genome-wide interspecies comparison. *Genome Research*, **16**, 875-884.
729 Harpur BA, Kent CF, Molodtsova D *et al.* (2014) Population genomics of the honey bee reveals
730 strong signatures of positive selection on worker traits. *Proceedings of the National Academy of*
731 *Sciences of the United States of America*, **111**, 2614–2619.

732 Haselkorn TS, Markow TA, Moran NA (2009) Multiple introductions of the *Spiroplasma* bacterial
733 endosymbiont into *Drosophila*. *Molecular Ecology*, **18**, 1294–1305.
734 Haudry A, Laurent S, Kapun M. 2020. Population Genomics on the Fly: Recent Advances in
735 Drosophila. In: Dutheil JY, editor. Statistical Population Genomics. Vol. 2090. New York, NY:
736 Springer US. p. 357–396.
737 Hewitt GM. (1999). Post-glacial re-colonization of European biota. *Biological Journal of the Linnean*
738 *Society* **68**:87–112.
739 Hijmans RJ, Cameron SE, Parra JL, Jones PG, Jarvis A. 2005. Very high resolution interpolated
740 climate surfaces for global land areas. *Int. J. Climatol*. 25:1965–1978.
741 Hohenlohe PA, Bassham S, Etter PD *et al.* (2010) Population Genomics of Parallel Adaptation in
742 Threespine Stickleback using Sequenced RAD Tags. *PLoS Genetics*, **6**, e1000862.
743 Hoffmann AA, Weeks AR (2007) Climatic selection on genes and traits after a 100 year-old invasion:
744 a critical look at the temperate-tropical clines in *Drosophila melanogaster* from eastern Australia.
745 *Genetica*, **129**, 133–147.
746 Huang DW, Sherman BT, Lempicki RA (2009) Systematic and integrative analysis of large gene lists
747 using DAVID bioinformatics resources. *Nature Protocols,* **4**, 44–57.
748 Hudson RR, Kreitman M, Aguadé M (1987) A test of neutral molecular evolution based on nucleotide
749 data. *Genetics*, **116**, 153–159.
750 Hutter S, Li H, Beisswanger S, De Lorenzo D, Stephan W (2007) Distinctly Different Sex Ratios in
751 African and European Populations of *Drosophila melanogaster* Inferred From Chromosomewide
752 Single Nucleotide Polymorphism Data. *Genetics*, **177**, 469–480.
753 Kaminker, J.S., Bergman, C.M., Kronmiller, B. *et al.* (2002) The transposable elements of
754 the *Drosophila melanogaster* euchromatin: a genomics perspective. *Genome Biol.*,
755 **3**, research0084.
756 Kao JY, Zubair A, Salomon MP, Nuzhdin SV, Campo D (2015) Population genomic analysis
757 uncovers African and European admixture in *Drosophila melanogaster* populations from the
758 south-eastern United States and Caribbean Islands. *Molecular Ecology*, **24**, 1499–1509.

759 Kapopoulou A, Kapun M, Pavlidis P, *et al*. (2018a) Early split between African and European
760 populations of *Drosophila melanogaster*. Preprint at *bioRxiv*, doi: https://doi.org/10.1101/340422
761 Kapopoulou A, Pfeifer S, Jensen J, Laurent S (2018b). The demographic history of African
762 *Drosophila melanogaster*. Preprint at *bioRxiv*, doi:10.1101/340406
763 Kapun M, Flatt T (2019) The adaptive significance of chromosomal inversion polymorphisms in
764 *Drosophila melanogaster*. *Molecular Ecology*, **28**, 1263-1282
765 Kapun M, Fabian DK, Goudet J, Flatt T (2016a) Genomic Evidence for Adaptive Inversion Clines in
766 *Drosophila melanogaster*. *Molecular Biology and Evolution*, **33**, 1317–1336.
767 Kapun M, Schmidt C, Durmaz E, Schmidt PS, Flatt T (2016b) Parallel effects of the inversion
768 *In(3R)Payne* on body size across the North American and Australian clines in *Drosophila*
769 *melanogaster*. *Journal of Evolutionary Biology*, **29**, 1059–1072.
770 Kapun M, van Schalkwyk H, McAllister B, Flatt T, Schlötterer C (2014) Inference of chromosomal
771 inversion dynamics from Pool-Seq data in natural and laboratory populations of *Drosophila*
772 *melanogaster*. *Molecular Ecology*, **23**, 1813–1827.
773 Keller A (2007) *Drosophila melanogaster*'s history as a human commensal. *Current Biology*, **17**,
774 R77–R81.
775 Kennington JW, Partridge L, Hoffmann AA (2006) Patterns of Diversity and Linkage Disequilibrium
776 Within the Cosmopolitan Inversion *In(3R)Payne* in *Drosophila melanogaster* Are Indicative of
777 Coadaptation. *Genetics*, **172**, 1655 – 1663.
778 Kimura M (1984) *The Neutral Theory of Molecular Evolution*. Cambridge University Press.
779 Knibb WR, Oakeshott JG, Gibson JB (1981) Chromosome Inversion Polymorphisms in *Drosophila*
780 *melanogaster*. I. Latitudinal Clines and Associations between Inversions in Australasian
781 Populations. *Genetics*, **98**, 833–847.
782 Knief U, Bossu CM, Saino N, Hansson B, Poelstra J, Vijay N, Weissensteiner M, Wolf JBW. (2019).
783 Epistatic mutations under divergent selection govern phenotypic variation in the crow hybrid
784 zone. *Nat Ecol Evol*, **3**, 570–576.
785 Kofler R, Schlötterer C (2012) GOwinda: Unbiased analysis of gene set enrichment for genome-wide
786 association studies. *Bioinformatics*, **28**, 2084-2085.

787 Kofler R, Betancourt AJ, Schlötterer C (2012) Sequencing of pooled DNA samples (Pool-Seq)
788 uncovers complex dynamics of transposable element insertions in *Drosophila melanogaster.*
789 *PLoS Genetics*, **8**, e1002487.
790 Kofler R, Orozco-terWengel P, De Maio N *et al.* (2011) PoPoolation: A Toolbox for Population
791 Genetic Analysis of Next Generation Sequencing Data from Pooled Individuals. *PLoS ONE*, **6**,
792 e15925.
793 Kolaczkowski B, Kern AD, Holloway AK, Begun DJ (2011) Genomic Differentiation Between
794 Temperate and Tropical Australian Populations of *Drosophila melanogaster*. *Genetics*, **187**, 245–
795 260.
796 Kreitman M (1983) Nucleotide polymorphism at the alcohol dehydrogenase locus of *Drosophila*
797 *melanogaster*. *Nature*, **304**, 412–417.
798 Kriesner P, Conner WR, Weeks AR, Turelli M, Hoffmann AA (2016) Persistence of a *Wolbachia*
799 infection frequency cline in *Drosophila melanogaster* and the possible role of reproductive
800 dormancy. *Evolution*, **70**, 979–997.
801 Lachaise D, Cariou M-L, David JR *et al.* (1988) Historical Biogeography of the *Drosophila*
802 *melanogaster* Species Subgroup. In Hecht MK, Wallace B, Prance GT (Eds.) *Evolutionary*
803 *Biology* (pp. 159–225) Boston: Springer.
804 Lack JB, Cardeno CM, Crepeau MW *et al.* (2015) The *Drosophila* genome nexus: a population
805 genomic resource of 623 *Drosophila melanogaster* genomes, including 197 from a single
806 ancestral range population. *Genetics*, **199**, 1229–1241.
807 Lack JB, Lange JD, Tang AD, Corbett-Detig RB, Pool JE (2016) A Thousand Fly Genomes: An
808 Expanded *Drosophila* Genome Nexus. *Molecular Biology and Evolution*, **33**, 3308–3313.
809 Langley CH, Stevens K, Cardeno C *et al.* (2012) Genomic variation in natural populations of
810 *Drosophila melanogaster*. *Genetics*, **192**, 533–598.
811 Larracuente AM, Roberts DM (2015) Genetics on the Fly: A Primer on the *Drosophila* Model
812 System. *Genetics* **201**, 815–842.
813 Lawrie DS, Messer PW, Hershberg R, Petrov DA (2013) Strong Purifying Selection at Synonymous
814 Sites in *D. melanogaster*. *PLoS Genetics,* **9**, e1003527.

Lerat E, Goubert C, Guirao-Rico S, Merenciano M, Dufour A-B, Vieira C, González J (2019) Population-specific dynamics and selection patterns of transposable element insertions in European natural populations. *Molecular Ecology*, **28**,1506–1522.

Lemeunier F, Aulard S (1992). Inversion polymorphism in *Drosophila melanogaster.* In: Krimbas CB, & Powell JR (Eds.), *Drosophila Inversion Polymorphism* (pp. 339–405), New York: CRC Press.

Lewontin RC (1974) *The Genetic Basis of Evolutionary Change*. Columbia University Press.

Li H, Ruan J, Durbin R (2008) Mapping short DNA sequencing reads and calling variants using mapping quality scores. *Genome Research*, **18**, 1851–1858.

Li H, Stephan W (2006) Inferring the Demographic History and Rate of Adaptive Substitution in *Drosophila*. PLoS Genetics **2**, 10.

Machado HE, Bergland AO, O'Brien KR *et al.* (2016) Comparative population genomics of latitudinal variation in *Drosophila simulans* and *Drosophila melanogaster*. *Molecular Ecology*, **25**, 723–740.

Machado H, Bergland AO, Taylor R *et al.* (2019) Broad geographic sampling reveals predictable, pervasive, and strong seasonal adaptation in *Drosophila*. Preprint at *bioRxiv*, doi: https://doi.org/10.1101/337543.

Macholán M, Baird SJ, Munclinger P, Dufková P, Bímová B, Piálek J. (2008). Genetic conflict outweighs heterogametic incompatibility in the mouse hybrid zone? *BMC Evolutionary Biology* **8**:271.

Martino ME, Ma D, Leulier F (2017) Microbial influence on *Drosophila* biology. *Current Opinion in Microbiology*, **38**, 165–170.

Mateo L, Rech GE, González J (2018) Genome-wide patterns of local adaptation in *Drosophila melanogaster*: adding intra European variability to the map. Preprint at *bioRxiv*, doi: https://doi.org/10.1101/269332

McDonald JH, Kreitman M (1991) Adaptive protein evolution at the *Adh* locus in *Drosophila*. *Nature*, **351**, 652–654.

842 Mettler LE, Voelker RA, Mukai T (1977) Inversion Clines in Populations of *Drosophila*
843 *melanogaster. Genetics*, **87**, 169–176.
844 Meyer F, Paarmann D, D'Souza M *et al.* (2008) The metagenomics RAST server - a public resource
845 for the automatic phylogenetic and functional analysis of metagenomes. *BMC Bioinformatics*, **9**,
846 386.
847 Michalakis Y, Veuille M (1996) Length variation of CAG/CAA trinucleotide repeats in natural
848 populations of *Drosophila melanogaster* and its relation to the recombination rate. *Genetics*, **143**,
849 1713–1725.
850 Nielsen R, Akey JM, Jakobsson M *et al.* (2017) Tracing the peopling of the world through genomics.
851 *Nature*, **541**, 302-310.
852 Novembre J, Johnson T, Bryc K, *et al.* (2008) Genes mirror geography within Europe. *Nature*, **456**,
853 98-101.
854 Paaby AB, Bergland AO, Behrman EL, Schmidt PS (2014) A highly pleiotropic amino acid
855 polymorphism in the *Drosophila* insulin receptor contributes to life-history adaptation. *Evolution*,
856 **68**, 3395-3409.
857 Paaby AB, Blacket MJ, Hoffmann AA, Schmidt PS (2010) Identification of a candidate adaptive
858 polymorphism for *Drosophila* life history by parallel independent clines on two continents.
859 *Molecular Ecology*, **19**, 760-774.
860 Palmer WH, Medd NC, Beard PM, Obbard DJ (2018) Isolation of a natural DNA virus of Drosophila
861 melanogaster, and characterisation of host resistance and immune responses. *PLOS Pathogens*,
862 **14**, e1007050
863 Parsch J, Novozhilov S, Saminadin-Peter SS, Wong KM, Andolfatto P (2010) On the utility of short
864 intron sequences as a reference for the detection of positive and negative selection in *Drosophila*.
865 *Molecular Biology and Evolution*, **27**, 1226–1234.
866 Peel MC, Finlayson BL, McMahon TA (2007) Updated world map of the Köppen-Geiger climate
867 classification. *Hydrology and Earth System Sciences*, **11**, 1633–1644.

Petrov DA, Fiston-Lavier AS, Lipatov M, Lenkov K, González J (2011) Population Genomics of Transposable Elements in *Drosophila melanogaster*. *Molecular Biology and Evolution*, **28**, 1633–1644.

Pool JE, Braun DT, Lack JB (2016) Parallel Evolution of Cold Tolerance Within *Drosophila melanogaster*. *Molecular Biology and Evolution*, **34,** 349–360.

Pool JE, Corbett-Detig RB, Sugino RP *et al.* (2012) Population Genomics of Sub-Saharan *Drosophila melanogaster*: African Diversity and Non-African Admixture. *PLoS Genetics*, **8**, e1003080.

Powell JR (1997) *Progress and Prospects in Evolutionary Biology: The Drosophila Model*. Oxford University Press.

Quesneville H, Bergman CM, Andrieu O, Autard D, Nouaud D, et al. (2005) Combined evidence annotation of transposable elements in genome sequences. *PLoS Comp Biol* **1(2)**: e22.

Rako L, Anderson AR, Sgrò CM, Stocker AJ, Hoffmann AA (2006) The association between inversion *In(3R)Payne* and clinally varying traits in *Drosophila melanogaster. Genetica*, **128**, 373–384.

Rane RV, Rako L, Kapun M, LEE SF (2015) Genomic evidence for role of inversion *3RP* of *Drosophila melanogaster* in facilitating climate change adaptation. *Molecular Ecology*, **24**, 2423–2432.

Rech GE, Bogaerts-Márquez M, Barrón MG, Merenciano M, Villanueva-Cañas JL, Horváth V, Fiston-Lavier A-S, Luyten I, Venkataram S, Quesneville H, Petrov DA, González J (2019) Stress response, behavior, and development are shaped by transposable element-induced mutations in *Drosophila*. *PLOS Genetics,* **15**, e1007900.

Richardson MF, Weinert LA, Welch JJ *et al.* (2012) Population Genomics of the *Wolbachia* Endosymbiont in *Drosophila melanogaster. PLoS Genetics*, **8**, e1003129.

Rogers RL, Hartl DL (2012) Chimeric genes as a source of rapid evolution in *Drosophila melanogaster*. *Molecular Biology and Evolution*, **29**, 517–529.

Schlötterer C, Tobler R, Kofler R, Nolte V (2014) Sequencing pools of individuals - mining genome-wide polymorphism data without big funding. *Nature Reviews Genetics*, **15**, 749–763.

Schmidt PS, Paaby AB (2008) Reproductive Diapause and Life-History Clines in North American Populations of *Drosophila melanogaster*. *Evolution*, **62**, 1204–1215.

Schmidt PS, Zhu CT, Das J *et al.* (2008) An amino acid polymorphism in the *couch potato* gene forms the basis for climatic adaptation in *Drosophila melanogaster*. *Proceedings of the National Academy of Sciences of the United States of America*, **105**, 16207–16211.

Singh ND, Arndt PF, Clark AG, Aquadro CF (2009) Strong evidence for lineage and sequence specificity of substitution rates and patterns in *Drosophila*. *Molecular Biology and Evolution*, **26**, 1591–1605.

Sprengelmeyer QD, Mansourian S, Lange JD, Matute DR, Cooper BS, Jirle EV, Stensmyr MC, Pool JE. (2020). Recurrent Collection of Drosophila melanogaster from Wild African Environments and Genomic Insights into Species History. *Mol Biol Evol* **37**:627–638.

Staubach F, Baines JF, Künzel S, Bik EM, Petrov DA (2013) Host species and environmental effects on bacterial communities associated with *Drosophila* in the laboratory and in the natural environment. *PLoS ONE*, **8**, e70749.

Szymura JM, Barton NH. (1986). Genetic analysis of a hybrid zone between the fire-bellied toads, *Bombina bombina* and *B. variegata*, near Cracow in Southern Poland. *Evolution* **40**:1141–1159.

Tauber E, Zordan, M, Sandrelli F, Pegoraro M, Osterwalder N, Breda C, Daga A, Selmin A, Monger K, Benna C, Rosata E, Kyriacou CP, Costa R (2007) Natural selection favors a newly derived *timeless* allele in *Drosophila melanogaster*. *Science,* **316,**1895-1899.

Trinder M, Daisley BA, Dube JS, Reid G (2017) *Drosophila melanogaster* as a High-Throughput Model for Host-Microbiota Interactions. *Frontiers in Microbiology*, **8**, 751.

Turner TL, Levine MT, Eckert ML, Begun DJ (2008) Genomic analysis of adaptive differentiation in *Drosophila melanogaster*. *Genetics*, **179**, 455–473.

Umina PA, Weeks AR, Kearney MR, McKechnie SW, Hoffmann AA (2005) A rapid shift in a classic clinal pattern in *Drosophila* reflecting climate change. *Science*, **308**, 691–693.

Unckless RL (2011) A DNA virus of *Drosophila*. *PLoS ONE*, **6**, e26564.

de Villemereuil P, Gaggiotti OE (2015) A new FST-based method to uncover local adaptation using environmental variables. *Methods in Ecology and Evolution*. **6**: 1248 – 1258.

Walters AM, Matthews MK, Hughes R, Malcolm Jaanna, Rudman S, Newell PD, Douglas AE, Schmidt PS, Chaston JM (2018) The microbiota influences the Drosophila melanogaster life history strategy. bioRxiv. 471540

Wang Y, Kapun M, Waidele L, Kuenzel S, Bergland AO, Staubach F. (2020). Common structuring principles of the *Drosophila melanogaster* microbiome on a continental scale and between host and substrate. Environmental Microbiology Reports **12**:220–228.

Wang Y, Staubach F (2018); Individual variation of natural *D.melanogaster*-associated bacterial communities, *FEMS Microbiology Letters*, **365**, fny017

Webster CL, Longdon B, Lewis SH, Obbard DJ (2016) Twenty-Five New Viruses Associated with the Drosophilidae (Diptera). *Evolutionary Bioinformatics Online*, **12**, 13–25.

Webster CL, Waldron FM, Robertson S *et al.* (2015) The Discovery, Distribution, and Evolution of Viruses Associated with *Drosophila melanogaster. PLoS Biology*, **13**, e1002210.

Werren JH, Baldo L, Clark ME (2008) Wolbachia: master manipulators of invertebrate biology. *Nature Reviews Microbiology*, **6**, 741–751.

Whitlock MC, McCauley DE (1999) Indirect measures of gene flow and migration: $F_{ST} \neq 1/(4Nm+1)$. Heredity, **82**,117–125.

Wilfert L, Longdon B, Ferreira AGA, Bayer F, Jiggins FM (2011) Trypanosomatids are common and diverse parasites of *Drosophila*. *Parasitology*, **138**, 858–865.

Wolff JN, Camus MF, Clancy DJ, Dowling DK (2016) Complete mitochondrial genome sequences of thirteen globally sourced strains of fruit fly (*Drosophila melanogaster*) form a powerful model for mitochondrial research. *Mitochondrial DNA Part A,* **27**, 4672–4674.

Wright S (1951) The genetical structure of populations. *Ann Eugen* **15**, 323–354.

Xiao F-X, Yotova V, Zietkiewicz E *et al.* (2004) Human *X*-chromosomal lineages in Europe reveal Middle Eastern and Asiatic contacts. *European Journal of Human Genetics*, **12**, 301–311.

Yukilevich R, True JR (2008a) Incipient sexual isolation among cosmopolitan *Drosophila melanogaster* populations. *Evolution*, **62**, 2112–2121.

Yukilevich R, True JR (2008b) African morphology, behavior and pheromones underlie incipient sexual isolation between us and Caribbean *Drosophila melanogaster. Evolution*, **62**, 2807–2828.

951 Zanini F, Brodin J, Thebo L *et al.* (2015) Population genomics of intrapatient HIV-1 evolution. *eLife*,
952 **4**, e11282.

953 **Tables**

954 **Table 1. Sample information for all populations in the *DrosEU* dataset.** Origin, collection date, season and sample size (number of chromosomes: *n*) of

955 the 48 samples in the *DrosEU* 2014 data set. Additional information can be found in supplementary table S1 (Supplementary Material online).

ID	Country	Location	Coll. Date	Numbe r ID	Lat (°)	Lon (°)	Alt (m)	Season	*n*	Coll. name
AT_Mau_14_01	Austria	Mauternbach	2014-07-20	1	48.38	15.56	572	S	80	Andrea J. Betancourt
AT_Mau_14_02	Austria	Mauternbach	2014-10-19	2	48.38	15.56	572	F	80	Andrea J. Betancourt
TR_Yes_14_03	Turkey	Yesiloz	2014-08-31	3	40.23	32.26	680	S	80	Banu Sebnem Onder
TR_Yes_14_04	Turkey	Yesiloz	2014-10-23	4	40.23	32.26	680	F	80	Banu Sebnem Onder
FR_Vil_14_05	France	Viltain	2014-08-18	5	48.75	2.16	153	S	80	Catherine Montchamp-Moreau
FR_Vil_14_07	France	Viltain	2014-10-27	7	48.75	2.16	153	F	80	Catherine Montchamp-Moreau
FR_Got_14_08	France	Gotheron	2014-07-08	8	44.98	4.93	181	S	80	Cristina Vieira
UK_She_14_09	United Kingdom	Sheffield	2014-08-25	9	53.39	-1.52	100	S	80	Damiano Porcelli

UK_Sou_14_10	United Kingdom	South Queensferry	2014-07-14	10	55.97	-3.35	19	S	80	Darren Obbard
CY_Nic_14_11	Cyprus	Nicosia	2014-08-10	11	35.07	33.32	263	S	80	Eliza Argyridou
UK_Mar_14_12	United Kingdom	Market Harborough	2014-10-20	12	52.48	-0.92	80	F	80	Eran Tauber
UK_Lut_14_13	United Kingdom	Lutterworth	2014-10-20	13	52.43	-1.10	126	F	80	Eran Tauber
DE_Bro_14_14	Germany	Broggingen	2014-06-26	14	48.22	7.82	173	S	80	Fabian Staubach
DE_Bro_14_15	Germany	Broggingen	2014-10-15	15	48.22	7.82	173	F	80	Fabian Staubach
UA_Yal_14_16	Ukraine	Yalta	2014-06-20	16	44.50	34.17	72	S	80	Iryna Kozeretska
UA_Yal_14_18	Ukraine	Yalta	2014-08-27	18	44.50	34.17	72	S	80	Iryna Kozeretska
UA_Ode_14_19	Ukraine	Odesa	2014-07-03	19	46.44	30.77	54	S	80	Iryna Kozeretska
UA_Ode_14_20	Ukraine	Odesa	2014-07-22	20	46.44	30.77	54	S	80	Iryna Kozeretska
UA_Ode_14_21	Ukraine	Odesa	2014-08-29	21	46.44	30.77	54	S	80	Iryna Kozeretska
UA_Ode_14_22	Ukraine	Odesa	2014-10-10	22	46.44	30.77	54	F	80	Iryna Kozeretska
UA_Kyi_14_23	Ukraine	Kyiv	2014-08-09	23	50.34	30.49	179	S	80	Iryna Kozeretska
UA_Kyi_14_24	Ukraine	Kyiv	2014-09-08	24	50.34	30.49	179	F	80	Iryna Kozeretska

UA_Var_14_25	Ukraine	Varva	2014-08-18	25	50.48	32.71	125	S	80	Oleksandra Protsenko
UA_Pyr_14_26	Ukraine	Pyriatyn	2014-08-20	26	50.25	32.52	114	S	80	Oleksandra Protsenko
UA_Dro_14_27	Ukraine	Drogobych	2014-08-24	27	49.33	23.50	275	S	80	Iryna Kozeretska
UA_Cho_14_28	Ukraine	Chornobyl	2014-09-13	28	51.37	30.14	121	F	80	Iryna Kozeretska
UA_Cho_14_29	Ukraine	Chornobyl Yaniv	2014-09-13	29	51.39	30.07	121	F	80	Iryna Kozeretska
SE_Lun_14_30	Sweden	Lund	2014-07-31	30	55.69	13.20	51	S	80	Jessica Abbott
DE_Mun_14_31	Germany	Munich	2014-06-19	31	48.18	11.61	520	S	80	John Parsch
DE_Mun_14_32	Germany	Munich	2014-09-03	32	48.18	11.61	520	F	80	John Parsch
PT_Rec_14_33	Portugal	Recarei	2014-09-26	33	41.15	-8.41	175	F	80	Jorge Vieira
ES_Gim_14_34	Spain	Gimenells (Lleida)	2014-10-20	34	41.62	0.62	173	F	80	Lain Guio
ES_Gim_14_35	Spain	Gimenells (Lleida)	2014-08-13	35	41.62	0.62	173	S	80	Lain Guio
FI_Aka_14_36	Finland	Akaa	2014-07-25	36	61.10	23.52	88	S	80	Maaria Kankare
FI_Aka_14_37	Finland	Akaa	2014-08-27	37	61.10	23.52	88	S	80	Maaria Kankare
FI_Ves_14_38	Finland	Vesanto	2014-07-26	38	62.55	26.24	121	S	66	Maaria Kankare
DK_Kar_14_39	Denmark	Karensminde	2014-09-01	39	55.95	10.21	15	F	80	Mads Fristrup Schou
DK_Kar_14_41	Denmark	Karensminde	2014-11-25	41	55.95	10.21	15	F	80	Mads Fristrup Schou
CH_Cha_14_42	Switzerland	Chalet à Gobet	2014-07-24	42	46.57	6.70	872	S	80	Martin Kapun

CH_Cha_14_43	Switzerland	Chalet à Gobet	2014-10-05	43	46.57	6.70	872	F	80	Martin Kapun
AT_See_14_44	Austria	Seeboden	2014-08-17	44	46.81	13.51	591	S	80	Martin Kapun
UA_Kha_14_45	Ukraine	Kharkiv	2014-07-26	45	49.82	36.05	141	S	80	Svitlana Serga
UA_Kha_14_46	Ukraine	Kharkiv	2014-09-14	46	49.82	36.05	141	F	80	Svitlana Serga
UA_Cho_14_47	Ukraine	Chornobyl Applegarden	2014-09-13	47	51.27	30.22	121	F	80	Svitlana Serga
UA_Cho_14_48	Ukraine	Chornobyl Polisske	2014-09-13	48	51.28	29.39	121	F	70	Svitlana Serga
UA_Kyi_14_49	Ukraine	Kyiv	2014-10-11	49	50.34	30.49	179	F	80	Svitlana Serga
UA_Uma_14_50	Ukraine	Uman	2014-10-01	50	48.75	30.21	214	F	80	Svitlana Serga
RU_Val_14_51	Russia	Valday	2014-08-17	51	57.98	33.24	217	S	80	Elena Pasyukova

956

Table 2. Clinality of genetic variation and population structure. Effects of geographic variables and/or seasonality on genome-wide average levels of diversity (π, θ and Tajima's D; top rows) and on the first three axes of a PCA based on allele frequencies at neutrally evolving sites (bottom rows). The values represent F-ratios from general linear models. Bold type indicates F-ratios that are significant after Bonferroni correction (adjusted α'=0.0055). Asterisks in parentheses indicate significance when accounting for spatial autocorrelation by spatial error models. These models were only calculated when Moran's I test, as shown in the last column, was significant. *$p < 0.05$; **$p < 0.01$; ***$p < 0.001$.

Factor	***Latitude***	***Longitude***	***Altitude***	***Season***	***Moran's I***
$\pi_{(X)}$	4.11*	1.62	**15.23*** **	1.65	0.86
$\pi_{(Aut)}$	0.91	2.54	**27.18*** **	0.16	-0.86
$\theta_{(X)}$	2.65	1.31	**15.54*** **	2.22	0.24
$\theta_{(Aut)}$	0.48	1.44	**13.66*** **	0.37	-1.13
$D_{(X)}$	0.02	0.38	5.93*	3.26	-2.08
$D_{(Aut)}$	0.09	0.76	5.33*	0.71	-1.45
PC1	0.63	**118.08*** **(*** **)**	3.64	0.75	**4.2*** **
PC2	**4.69***	**7.15***	**11.77*** *	1.68	-0.32
PC3	0.39	0.23	**19.91*** **	0.28	1.38

964 **Table 3**. **Clinality and/or seasonality of chromosomal inversions.** The values represent *F*-ratios from binomial generalized linear models to account for
965 frequency data. Bold type indicates deviance values that were significant after Bonferroni correction (adjusted α'=0.0071). Asterisks in parentheses indicate
966 significance when accounting for spatial autocorrelation by spatial error models. These models were only calculated when Moran's *I* test, as shown in the last
967 column, was significant. *$p < 0.05$; **$p < 0.01$; ***$p < 0.001$
968

Factor	***Latitude***	***Longitude***	***Altitude***	***Season***	***Moran's I***
In(2L)t	2.2	**10.09****	**43.94*****	0.89	-0.92
In(2R)NS	0.25	**14.43*****	2.88	2.43	1.25
In(3L)P	**21.78*****	2.82	0.62	3.6	-1.61
In(3R)C	**18.5***(***)**	0.75	1.42	0.04	2.79**
In(3R)Mo	0.3	0.09	0.35	0.03	-0.9
In(3R)Payne	**43.47*****	0.66	1.69	1.55	-0.89

969

970 **FIGURE LEGENDS**

971

972 **Fig. 1. The geographic distribution of population samples.** Locations of all samples in the 2014
973 *DrosEU* data set. The color of the circles indicates the sampling season for each location: ten of the
974 32 locations were sampled at least twice, once in summer and once in fall (see table 1 and
975 supplementary table S1, Supplementary Material online). Note that some of the 12 Ukrainian
976 locations overlap in the map.

977

978 **Fig. 2**. **Candidate signals of selective sweeps in European populations.** The central panel shows
979 the distribution of Tajima's *D* in 50 kb sliding windows with 40 kb overlap, with red and green
980 dashed lines indicating Tajima's $D = 0$ and -1, respectively. The top panel shows a detail of a genomic
981 region on chromosomal arm *2R* in the vicinity of *Cyp6g1* and *Hen1* (highlighted in red), genes
982 reportedly involved in pesticide resistance. This strong sweep signal is characterized by an excess of
983 low-frequency SNP variants and overall negative Tajima's *D* in all samples. Colored solid lines depict
984 Tajima's *D* for each sample (see supplementary fig. S2 for color codes, Supplementary Material
985 online); the black dashed line shows Tajima's *D* averaged across all samples. The bottom panel shows
986 a region on *3L* previously identified as a potential target of selection, which shows a similar strong
987 sweep signature. Notably, both regions show strongly reduced genetic variation (supplementary fig.
988 S1, Supplementary Material online).

989

990 **Fig. 3. Genetic differentiation among European populations**. (A) Average F_{ST} among populations
991 at putatively neutral sites. The centre plot shows the distribution of F_{ST} values for all 1,128 pairwise
992 population comparisons, with the F_{ST} values for each comparison obtained from the mean across all
993 4,034 SNPs used in the analysis. Plots on the left and the right show population pairs in the lower
994 (blue) and upper (red) 5% tails of the F_{ST} distribution. (B) PCA analysis of allele frequencies at the
995 same SNPs reveals population sub-structuring in Europe. Hierarchical model fitting using the first
996 four PCs showed that the populations fell into two clusters (indicated by red and blue), with cluster
997 assignment of each population subsequently estimated by *k*-means clustering. (C) Admixture

proportions for each population inferred by model-based clustering with *ConStruct* are highlighted as pie charts (left plot) or Structure plots (centre). The optimal number of 3 spatial layers (K) was inferred by cross-validation (right plot).

Fig. 4. Manhattan plots of SNPs with *q*-values < 0.05 in BayeScEnv association tests with PC1 or PC2 of bioclimatic variables. Vertical lines denote the breakpoints of common inversions. The gene names highlight some candidate genes found in our study and which have previously been identified as varying clinally by Fabian *et al*. (2012) and Machado *et al.* (2016) along the North American east coast. Note that *q*-values of 0 (which are infinite on a log-scale) are plotted at the top of each figure, above the grey dash-dotted horizontal lines in order to separate them from the other candidates with *q*-values > 0. These zero values are unlikely to be spurious as the densities of these infinite values tend to line up with peaks of $\log_{10}(q)$ below the dashed line, suggesting that they represent highly significant continuations of these peaks.

Fig. 5. Mitochondrial haplotypes. (A) TCS network showing the relationship of 5 common mitochondrial haplotypes; (B) estimated frequency of each mitochondrial haplotype in 48 European samples.

Fig. 6. Geographic patterns of structural variants. The upper panel shows stacked bar plots with the relative abundances of transposable elements (TEs) in all 48 population samples**.** The proportion of each repeat class was estimated from sampled reads with dnaPipeTE (2 samples per run, 0.1X coverage per sample). The lower panel shows stacked bar plots depicting absolute frequencies of six cosmopolitan inversions in all 48 population samples.

Fig. 7. Microbiota associated with *Drosophila*. Relative abundance of *Drosophila*-associated microbes as assessed by MGRAST classified shotgun sequences. Microbes had to reach at least 3% relative abundance in one of the samples to be represented

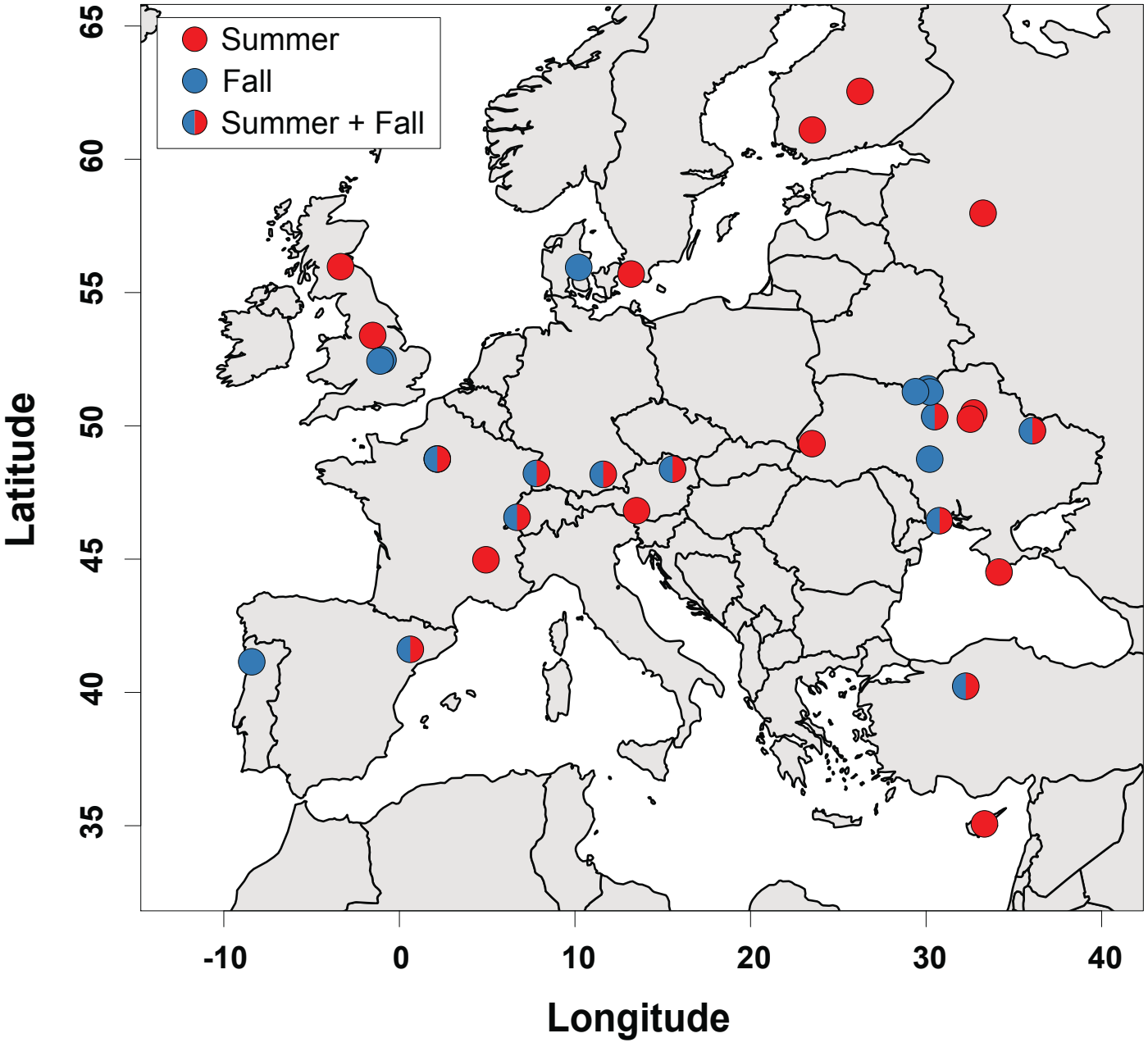
Summer
Fall
Summer + Fall
Latitude
65
60
55
50
45
40
35
-10
0
10
20
30
40
Longitude

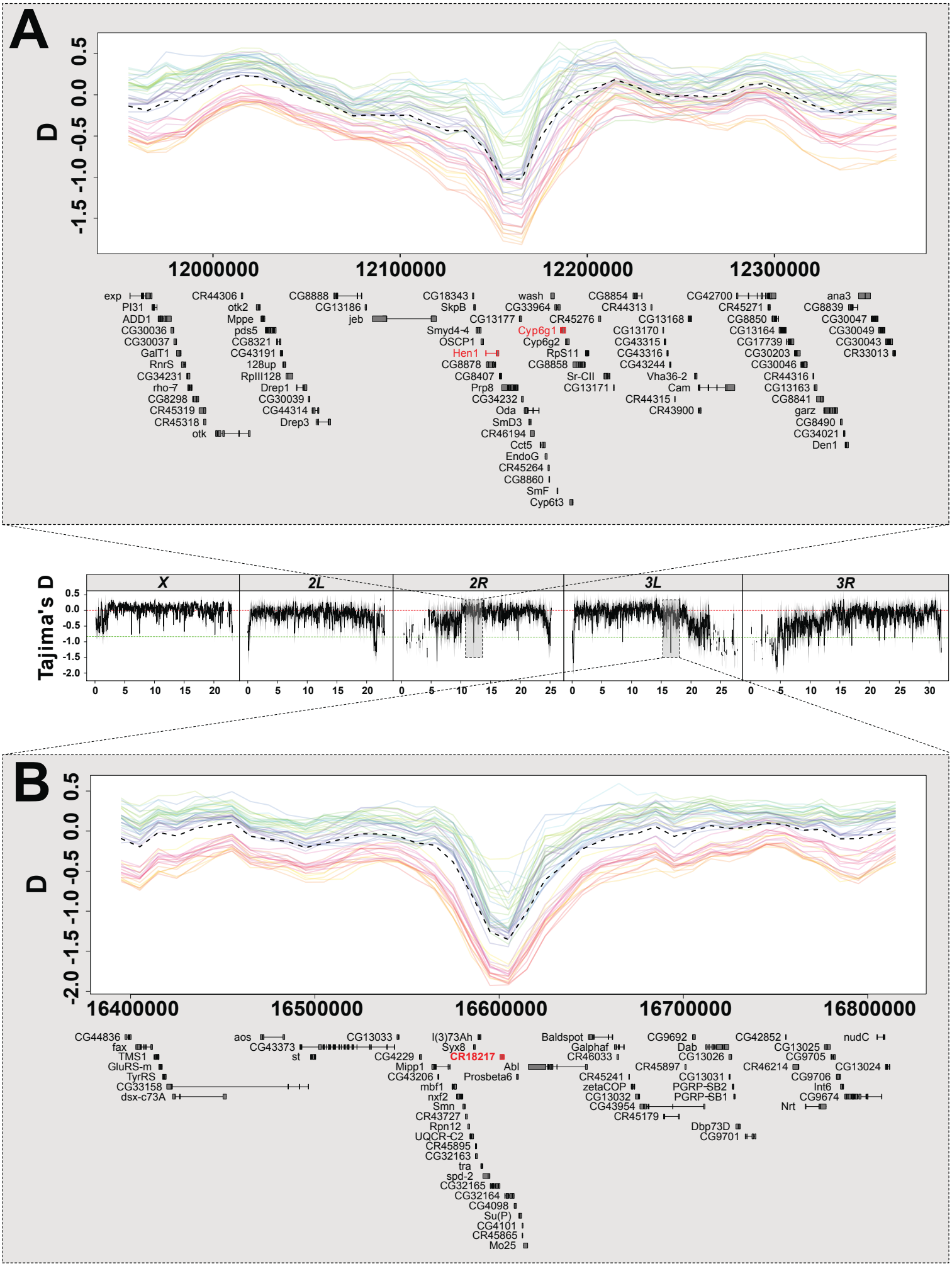
A
D
0.5
0.0
-0.5
-1.0
-1.5
12000000
12100000
12200000
12300000
exp
PI31
ADD1
CG30036
CG30037
GalT1
RnrS
CG34231
rho-7
CG8298
CR45319
CR45318
otk
CR44306
otk2
Mppe
pds5
CG8321
CG43191
128up
RpIII128
Drep1
CG30039
CG44314
Drep3
CG8888
CG13186
jeb
CG18343
SkpB
CG13177
Smyd4-4
OSCP1
Hen1
CG8878
CG8407
Prp8
CG34232
Oda
SmD3
CR46194
Cct5
EndoG
CR45264
CG8860
SmF
Cyp6t3
wash
CG33964
CR45276
Cyp6g1
Cyp6g2
RpS11
CG8858
Sr-CII
CG13171
CG8854
CR44313
CG13168
CG13170
CG43315
CG43316
CG43244
Vha36-2
Cam
CR44315
CR43900
CG42700
CR45271
CG8850
CG13164
CG17739
CG30203
CG30046
CR44316
CG13163
CG8841
garz
CG8490
CG34021
Den1
ana3
CG8839
CG30047
CG30049
CG30043
CR33013
Tajima's D
X
2L
2R
3L
3R
0.5
0.0
-0.5
-1.0
-1.5
-2.0
0
5
10
15
20
25
30
B
D
0.5
0.0
-0.5
-1.0
-1.5
-2.0
16400000
16500000
16600000
16700000
16800000
CG44836
fax
TMS1
GluRS-m
TyrRS
CG33158
dsx-c73A
aos
CG43373
st
CG13033
CG4229
Mipp1
CG43206
mbf1
nxf2
Smn
CR43727
Rpn12
UQCR-C2
CR45895
CG32163
tra
spd-2
CG32165
CG32164
CG4098
Su(P)
CG4101
CR45865
Mo25
l(3)73Ah
Syx8
CR18217
Abl
Prosbeta6
Baldspot
Galphaf
CR46033
CR45241
zetaCOP
CG13032
CG43954
CR45179
CG9692
Dab
CG13026
CR45897
CG13031
PGRP-SB2
PGRP-SB1
Dbp73D
CG9701
CG42852
CG13025
CG9705
CR46214
CG9706
Int6
CG9674
Nrt
nudC
CG13024

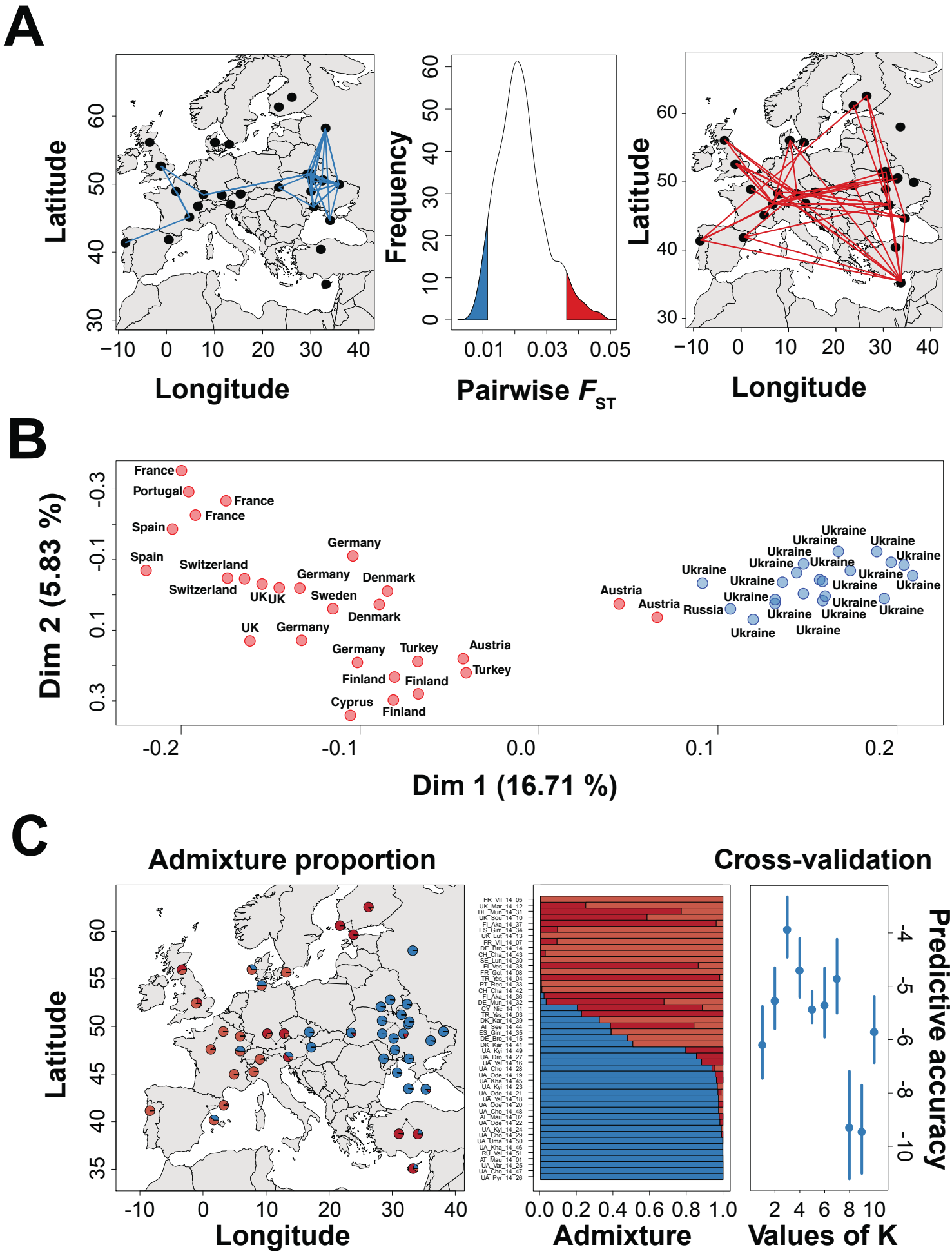
A
Latitude
Longitude
Frequency
Pairwise F_{ST}
B
Dim 2 (5.83 %)
Dim 1 (16.71 %)
France
Portugal
Spain
Switzerland
Germany
Denmark
Sweden
UK
Finland
Cyprus
Turkey
Austria
Russia
Ukraine
C
Admixture proportion
Cross-validation
Admixture
Values of K
Predictive accuracy

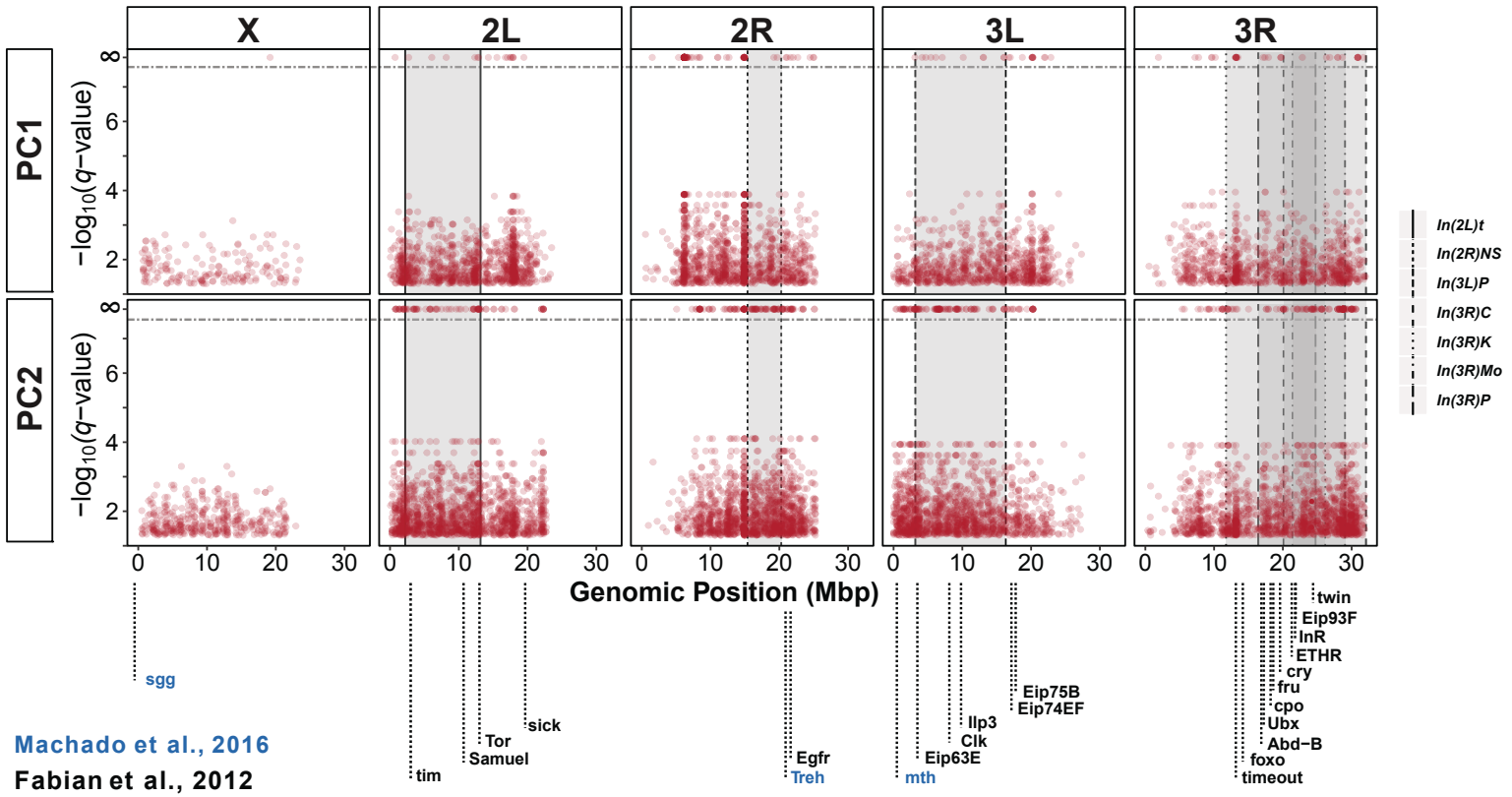

Machado et al., 2016

Fabian et al., 2012

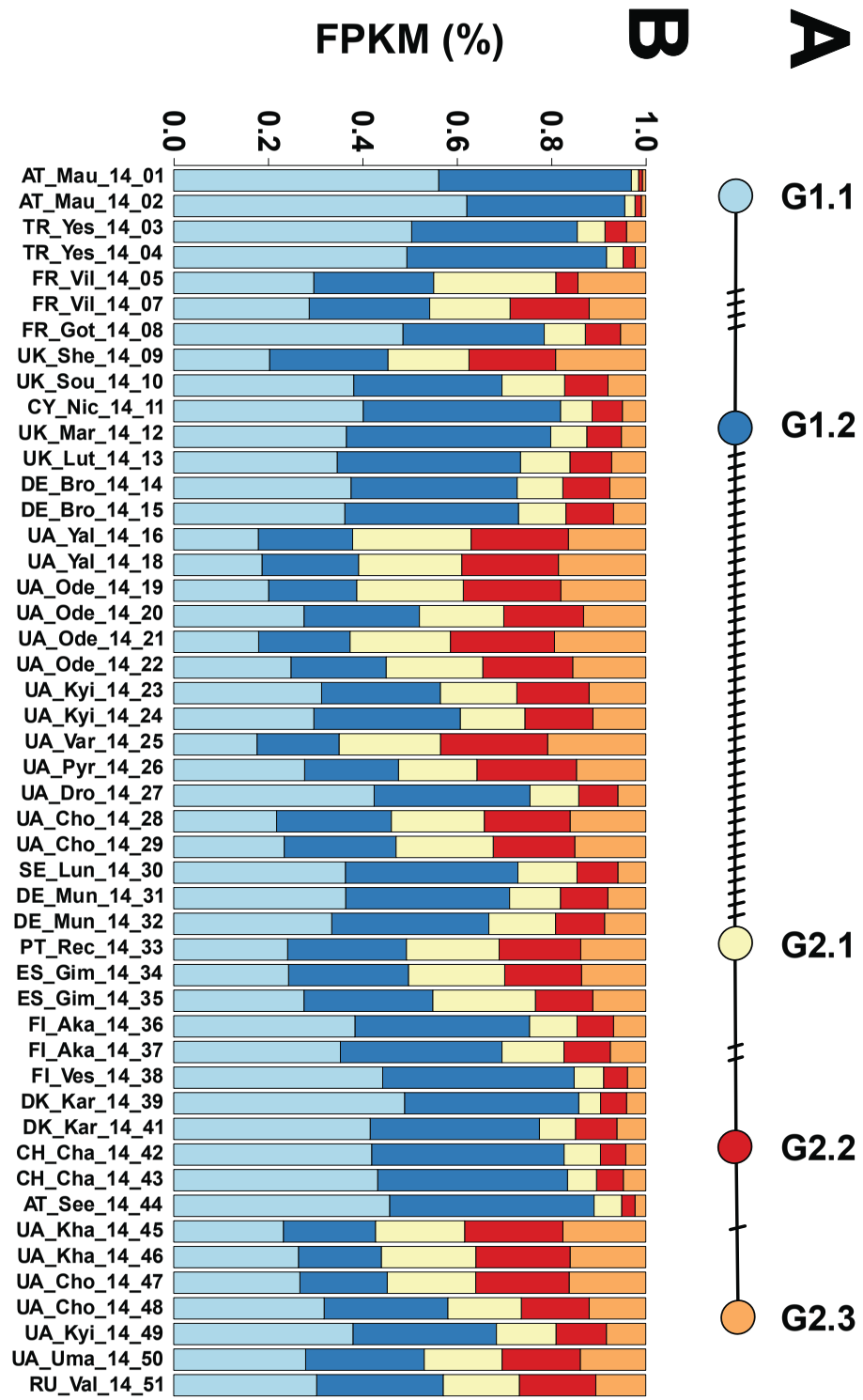
FPKM (%)
B
A
0.0
0.2
0.4
0.6
0.8
1.0
AT_Mau_14_01
AT_Mau_14_02
TR_Yes_14_03
TR_Yes_14_04
FR_Vil_14_05
FR_Vil_14_07
FR_Got_14_08
UK_She_14_09
UK_Sou_14_10
CY_Nic_14_11
UK_Mar_14_12
UK_Lut_14_13
DE_Bro_14_14
DE_Bro_14_15
UA_Yal_14_16
UA_Yal_14_18
UA_Ode_14_19
UA_Ode_14_20
UA_Ode_14_21
UA_Ode_14_22
UA_Kyi_14_23
UA_Kyi_14_24
UA_Var_14_25
UA_Pyr_14_26
UA_Dro_14_27
UA_Cho_14_28
UA_Cho_14_29
SE_Lun_14_30
DE_Mun_14_31
DE_Mun_14_32
PT_Rec_14_33
ES_Gim_14_34
ES_Gim_14_35
FI_Aka_14_36
FI_Aka_14_37
FI_Ves_14_38
DK_Kar_14_39
DK_Kar_14_41
CH_Cha_14_42
CH_Cha_14_43
AT_See_14_44
UA_Kha_14_45
UA_Kha_14_46
UA_Cho_14_47
UA_Cho_14_48
UA_Kyi_14_49
UA_Uma_14_50
RU_Val_14_51
G1.1
G1.2
G2.1
G2.2
G2.3

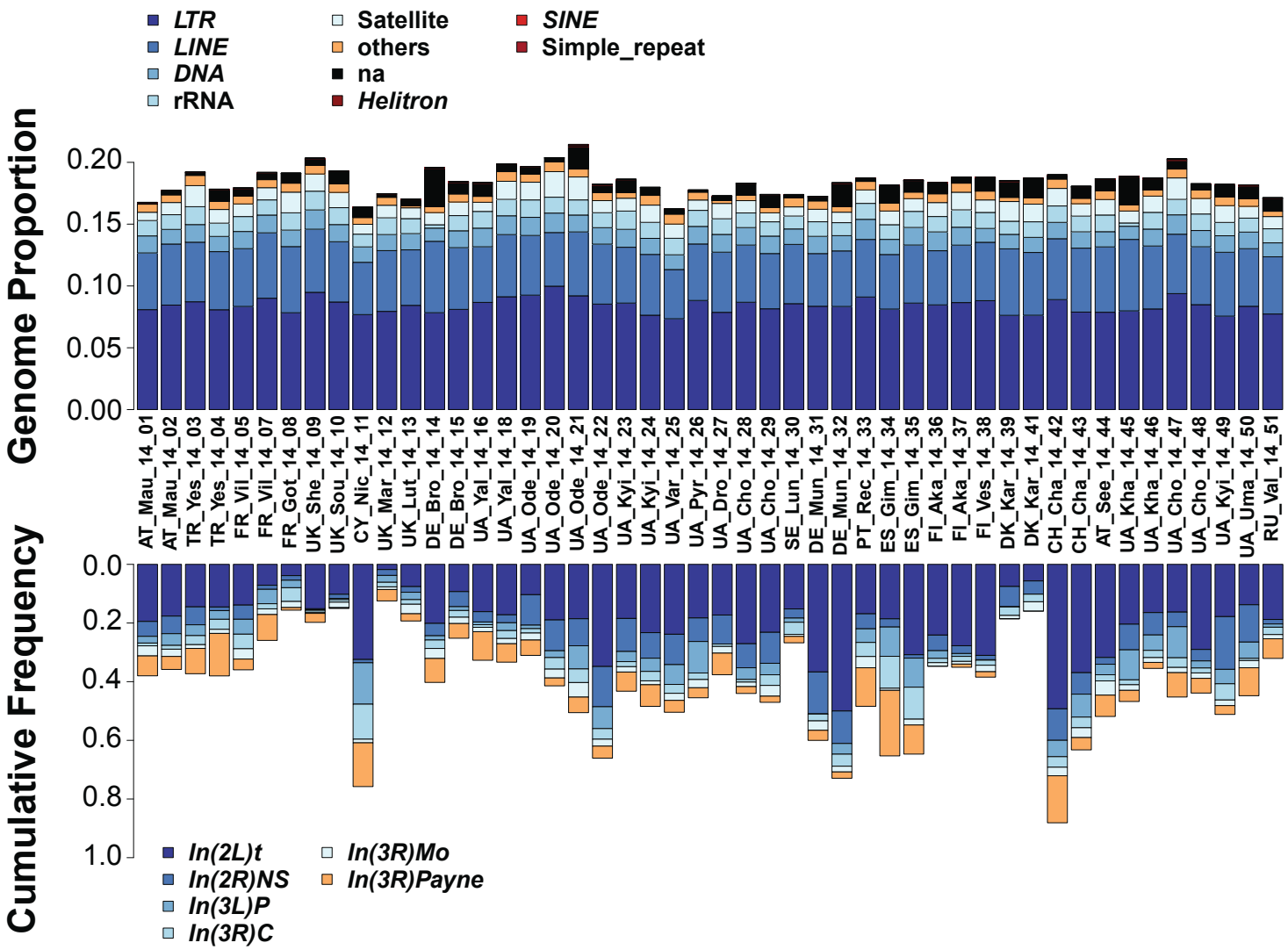
LTR
LINE
DNA
rRNA
Satellite
others
na
Helitron
SINE
Simple_repeat
Genome Proportion
0.20
0.15
0.10
0.05
0.00
AT_Mau_14_01
AT_Mau_14_02
TR_Yes_14_03
TR_Yes_14_04
FR_Vil_14_05
FR_Vil_14_07
FR_Got_14_08
UK_She_14_09
UK_Sou_14_10
CY_Nic_14_11
UK_Mar_14_12
UK_Lut_14_13
DE_Bro_14_14
DE_Bro_14_15
UA_Yal_14_16
UA_Yal_14_18
UA_Ode_14_19
UA_Ode_14_20
UA_Ode_14_21
UA_Ode_14_22
UA_Kyi_14_23
UA_Kyi_14_24
UA_Var_14_25
UA_Pyr_14_26
UA_Dro_14_27
UA_Cho_14_28
UA_Cho_14_29
SE_Lun_14_30
DE_Mun_14_31
DE_Mun_14_32
PT_Rec_14_33
ES_Gim_14_34
ES_Gim_14_35
FI_Aka_14_36
FI_Aka_14_37
FI_Ves_14_38
DK_Kar_14_39
DK_Kar_14_41
CH_Cha_14_42
CH_Cha_14_43
AT_See_14_44
UA_Kha_14_45
UA_Kha_14_46
UA_Cho_14_47
UA_Cho_14_48
UA_Kyi_14_49
UA_Uma_14_50
RU_Val_14_51
Cumulative Frequency
0.0
0.2
0.4
0.6
0.8
1.0
In(2L)t
In(2R)NS
In(3L)P
In(3R)C
In(3R)Mo
In(3R)Payne

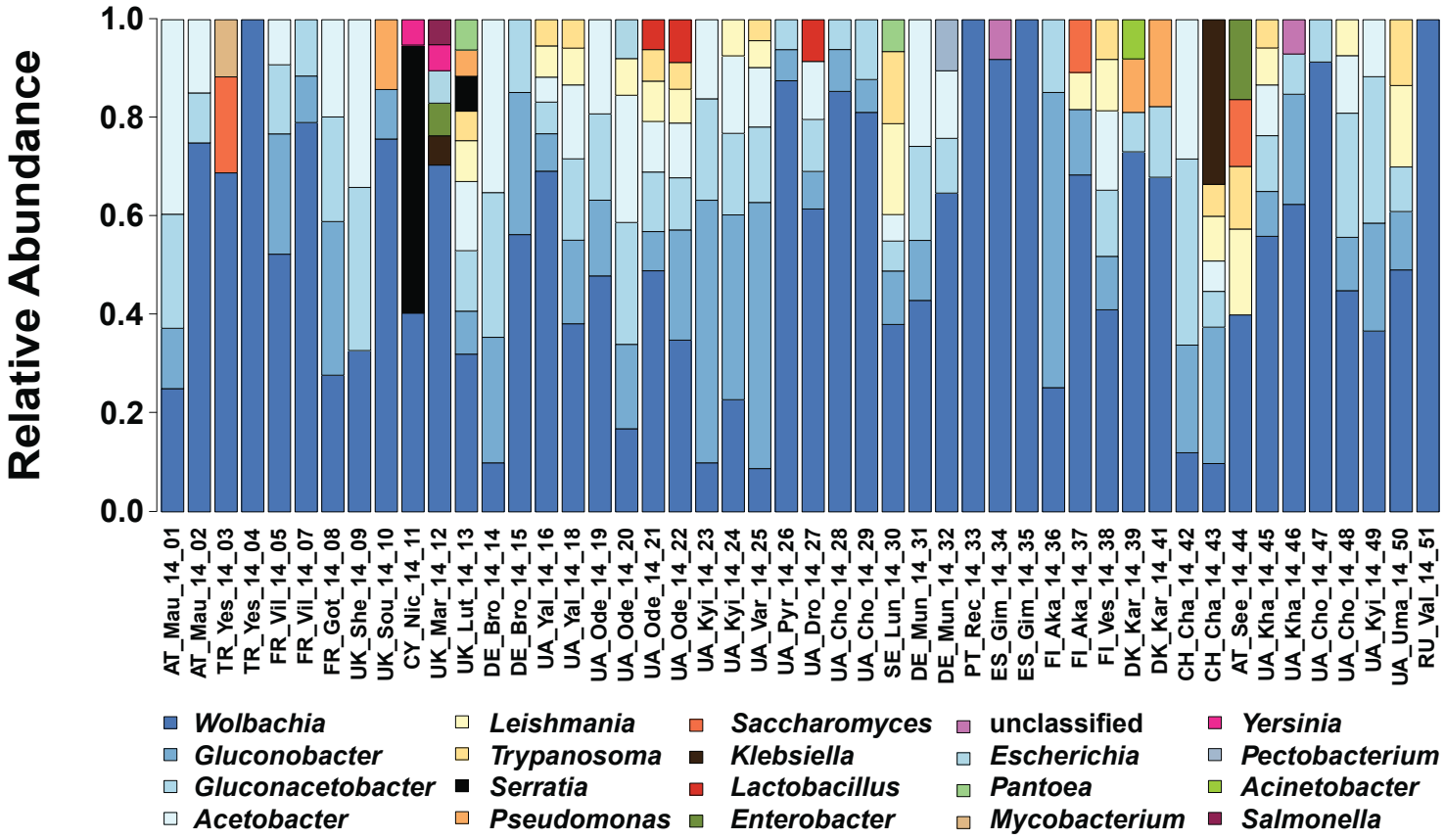
Relative Abundance
1.0
0.8
0.6
0.4
0.2
0.0
AT_Mau_14_01
AT_Mau_14_02
TR_Yes_14_03
TR_Yes_14_04
FR_Vil_14_05
FR_Vil_14_07
FR_Got_14_08
UK_She_14_09
UK_Sou_14_10
CY_Nic_14_11
UK_Mar_14_12
UK_Lut_14_13
DE_Bro_14_14
DE_Bro_14_15
UA_Yal_14_16
UA_Yal_14_18
UA_Ode_14_19
UA_Ode_14_20
UA_Ode_14_21
UA_Ode_14_22
UA_Kyi_14_23
UA_Kyi_14_24
UA_Var_14_25
UA_Pyr_14_26
UA_Dro_14_27
UA_Cho_14_28
UA_Cho_14_29
SE_Lun_14_30
DE_Mun_14_31
DE_Mun_14_32
PT_Rec_14_33
ES_Gim_14_34
ES_Gim_14_35
Fl_Aka_14_36
Fl_Aka_14_37
Fl_Ves_14_38
DK_Kar_14_39
DK_Kar_14_41
CH_Cha_14_42
CH_Cha_14_43
AT_See_14_44
UA_Kha_14_45
UA_Kha_14_46
UA_Cho_14_47
UA_Cho_14_48
UA_Kyi_14_49
UA_Uma_14_50
RU_Val_14_51
Wolbachia
Gluconobacter
Gluconacetobacter
Acetobacter
Leishmania
Trypanosoma
Serratia
Pseudomonas
Saccharomyces
Klebsiella
Lactobacillus
Enterobacter
unclassified
Escherichia
Pantoea
Mycobacterium
Yersinia
Pectobacterium
Acinetobacter
Salmonella